

XN-NF-80-19 (NP)

VOLUME 2A

**EXXON NUCLEAR METHODOLOGY FOR
BOILING WATER REACTORS -**

VOLUME 2A

**RELAX: A RELAP4 BASED COMPUTER CODE FOR
CALCULATING BLOWDOWN PHENOMENA**

JULY 1980

RICHLAND, WA 99352

EXXON NUCLEAR COMPANY, Inc.

8009260496

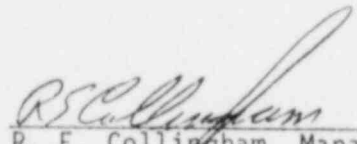
07/31/80

RELAX: A RELAP4 BASED COMPUTER
CODE FOR CALCULATING BLOWDOWN PHENOMENA

Prepared By

D. C. Kolesar

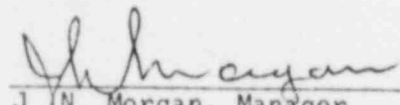
APPROVED:



R. E. Collingham, Manager
Systems Model Development

5/23/80
Date

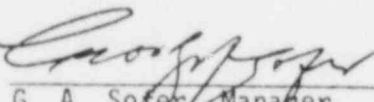
APPROVED:



J. N. Morgan, Manager
Licensing and Safety Engineering

5-27-80
Date

APPROVED:



G. A. Sofer, Manager
Nuclear Fuels Engineering

5-28-80
Date

May 1980

EXXON NUCLEAR COMPANY, Inc.

NUCLEAR REGULATORY COMMISSION DISCLAIMER

IMPORTANT NOTICE REGARDING CONTENTS AND USE OF THIS DOCUMENT

PLEASE READ CAREFULLY

This technical report was derived through research and development programs sponsored by Exxon Nuclear Company, Inc. It is being submitted by Exxon Nuclear to the USNRC as part of a technical contribution to facilitate safety analyses by licensees of the USNRC which utilize Exxon Nuclear-fabricated reload fuel or other technical services provided by Exxon Nuclear for light water power reactors and it is true and correct to the best of Exxon Nuclear's knowledge, information, and belief. The information contained herein may be used by the USNRC in its review of this report, and by licensees or applicants before the USNRC which are customers of Exxon Nuclear in their demonstration of compliance with the USNRC's regulations.

Without derogating from the foregoing, neither Exxon Nuclear nor any person acting on its behalf:

- A. Makes any warranty, express or implied, with respect to the accuracy, completeness, or usefulness of the information contained in this document, or that the use of any information, apparatus, method, or process disclosed in this document will not infringe privately owned rights; or
- B. Assumes any liabilities with respect to the use of, or for damages resulting from the use of, any information, apparatus, method, or process disclosed in this document.

KEY TO REPORT OF
EXXON NUCLEAR METHODOLOGY FOR BOILING WATER REACTORS
XN-NF-80-19

- Volume 1 Exxon Nuclear Methodology for Boiling Water Reactors -
 Neutronics Methods for Design and Analysis
- Volume 2 Exxon Nuclear Methodology for Boiling Water Reactors -
 EXEM: ECCS Evaluation Model, Summary Description
- Volume 2A RELAX: A RELAP4 Based Computer Code for Calculating
 Blowdown Phenomena
- Volume 2B FLEX: A Computer Code for Jet Pump BWR Refill and
 Reflood Analysis
- Volume 3 Exxon Nuclear Methodology for Boiling Water Reactors -
 Thermal Hydraulics

ACKNOWLEDGEMENT

The efforts of Donald S. Rowe and Associates in the development of the RELAX jet pump model and of D. C. Caraher of Intermountain Technologies Inc. in the programming of the new heat transfer regions are gratefully acknowledged.

TABLE OF CONTENTS

	<u>Page No.</u>
1.0 INTRODUCTION AND SUMMARY	1
2.0 DRIFT FLUX MODEL	3
2.1 ZUBER-FINDLAY EQUATION	3
2.2 FLOW REGIMES AND DRIFT FLUX CORRELATIONS	4
2.2.1 PROFILE SLIP, C_0	6
2.2.2 LOCAL SLIP, V_{gj}	7
2.3 CONSISTENCY WITH CCFL RELATIONS	10
2.4 VOID FRACTION SELECTION	12
2.5 DRIFT FLUX MODEL IMPLEMENTATION	13
2.5.1 BASIC EQUATIONS OF MOTION	14
2.5.2 DIFFERENCE EQUATIONS WITH DRIFT FLUX	15
2.5.3 ANATOMY OF DRIFT FLUX MODEL IN CODE	19
3.0 JET PUMP MODEL	26
3.1 JET PUMP NODING	27
3.2 STREAM TUBE MODELING	29
3.3 MIXING REGION EQUATIONS	31
3.4 NUMERICAL SOLUTION	35
3.5 IMPLEMENTATION OF JET PUMP MODEL IN RELAX	36
3.6 RELAX MODELING IN VICINITY OF JET PUMP	36
3.7 LOSS COEFFICIENTS	38

TABLE OF CONTENTS (Continued)

	<u>Page No.</u>
4.0 HEAT TRANSFER REGIMES	46
4.1 HEAT TRANSFER CORRELATIONS	46
4.1.1 CONDENSATION	46
4.1.2 NATURAL CONVECTION	48
4.1.3 POOL FILM BOILING	49
4.1.4 CONVECTIVE BOUNDARY CONDITION - MIXTURE LEVEL INTERACTION	50
4.2 RELAP4 UPDATES	50
5.0 NOMENCLATURE	51
5.1 NOMENCLATURE OF DRIFT FLUX SECTION (SECTION 2)	51
5.2 NOMENCLATURE OF JET PUMP SECTION (SECTION 3)	53
6.0 REFERENCES	55
APPENDIX A: VERIFICATION - RELAX PREDICTION OF EXPERIMENTAL BWR SYSTEM BEHAVIOR (TLTA)	A-1

LIST OF FIGURES

<u>Figure No.</u>		<u>Page No.</u>
2.1	RELAX Flow Regime Map for Drift Flux Correlations	21
2.2	Distribution Parameter Predicted by RELAX at 100 psia	22
2.3	Local Drift Velocity versus Void Fraction at 100 psia	23
2.4	Gas versus Liquid Volumetric Fluxes from Zuber-Findlay Equation at 100 psia	24
2.5	Two-Dimensional j_g - j_f Plane	25
3.1	Typical N-M Jet Pump Curve with Classification of Flow Types	39
3.2	RELAX Model of an Actual Jet Pump	40
3.3	Noding for Jet Pump Mixing Section and Illustration for Type 3+ Flow	41
3.4	Location of Variables in Jet Pump Model	42
3.5	Variable Placement for the Multinode Mixing Section	43
3.6	Jet Pump Loss Coefficients Obtained from EG&G Flow Tests	44
3.7	Comparison of Experimental and Calculated M-N Curve for EG&G Jet Pump Tests	45
A-1	Steam Dome Pressure - TLTA Test 6007	A-3
A-2	Core Inlet Flow - TLTA Test 6007	A-4
A-3	Lower Plenum Mass - TLTA Test 6007	A-5

1.0 INTRODUCTION AND SUMMARY

This document describes the RELAP4-based LOCA blowdown analysis code (RELAX). RELAP4-EM/ENC28B⁽¹⁾ has been the Exxon Nuclear Company blowdown computer program approved by the NRC⁽²⁾ for use in ECCS Evaluation Models on PWRs and NJP-BWRs. RELAX was developed by adding a slip flow model, a new jet pump model and additional heat transfer regimes to RELAP4-EM/ENC28B to improve blowdown prediction capabilities. As with RELAP4-EM/ENC28B, RELAX-EM complies with Appendix K requirements for ECCS analysis. Only the changes that separate RELAX from RELAP4-EM/ENC28B are discussed herein.

The modifications to RELAP4-EM/ENC28B are summarized as follows:

- A slip flow model has been introduced based on drift flux theory. This improves the capability of the code to predict two-phase flow phenomena. Slip flow permits thermal convection to be based upon liquid and gas velocities individually rather than on an equal velocity (homogeneous flow) basis. Slip flow is introduced into the equations of fluid motion through the energy conservation equation. The drift flux model is based on the Zuber-Findlay relation between liquid and gas velocities. Coefficients needed in the Zuber-Findlay relation are based upon empirical relations as organized by a modified Bennett flow regime map.
- A mechanistic jet pump model has been developed and included in RELAX. The model characterizes flow through the jet pump under all flow conditions. Equations of mass and momentum are solved in a nodal matrix with empiricism introduced through pressure loss coefficients.

- Three heat transfer regimes were added to provide improved system blowdown heat transfer predictions: condensation to evaluate isolation condenser performance, natural convection to allow modeling of steam generators in dual cycle BWR systems, and a pool film boiling correlation to better calculate heat transfer for low flow/low quality conditions.

Verification of RELAX to experimental Jet Pump BWR system behavior (TLTA) is presented in the Appendix. The good agreement between TLTA data and RELAX predictions demonstrated in the Appendix supports the use of RELAX as a blowdown code for evaluation model analyses of jet pump BWRs.

2.0 DRIFT FLUX MODEL

The drift flux model describes slip in two-phase flow through algebraic relations. The literature discloses an extensive and growing use of drift flux theory⁽³⁻¹¹⁾. A practical feature of drift flux is that both co-current and counter-current flow may be accommodated in computer codes which were originally developed assuming homogeneous coolant flow. Several computer codes used in ECCS analysis have incorporated drift flux consistent with this framework⁽¹²⁻¹⁵⁾.

2.1 ZUBER-FINDLAY EQUATION

The RELAX drift flux model uses the Zuber-Findlay relation⁽³⁾,

$$j_g = \alpha (C_0 j + V_{gj}) \quad (2.1)$$

where

$$j = j_g + j_f \quad (2.2)$$

and j , j_g and j_f are the total, gas and liquid superficial velocities, respectively. Cross-sectional averaging notation has been dropped from the above expressions. V_{gj} is known as the "local slip" or "drift velocity". It is a measure of the tendency of gas to rise in a liquid regardless of fluid motion. C_0 is known as the "distribution parameter" or "profile slip". It represents the effect of non-uniform phase velocity and non-uniform concentration profiles.

Equation 2.1 can be written as

$$j_g = \alpha (j + \bar{V}_{gj}) \quad (2.3)$$

where \bar{V}_{gj} is the mean transport drift velocity. Thus,

$$\bar{V}_{gj} = V_{gj} + (C_0 - 1)j .$$

The mean transport drift velocity is a composite of local (described by V_{gj}) and distribution (described by C_0) effects.

The basis for the RELAX drift flux model is the equation set that consists of the Zuber-Findlay equation (Equation 2.1 or 2.3), the relation between superficial velocities (Equation 2.2) and the conservation of mass at an axial location:

$$\rho_g j_g + \rho_f j_f = \rho j = G.$$

2.2 FLOW REGIMES AND DRIFT FLUX CORRELATIONS

The drift flux parameters, V_{gj} and C_0 , are functions of flow regime, pressure, and geometry. Dependency on void fraction occurs in dispersed systems. Further, V_{gj} is related to C_0 through the Zuber-Findlay and the mass conservation equations. Ohkawa and Lahey⁽⁹⁾ have developed relations for V_{gj} and C_0 which fit drift flux data over the range of applicable reactor void and pressure conditions and are consistent with flooding limitations. Flooding is the term given to the phenomena that limits the downward flow of liquid against counter current updrafting steam.

RELAX uses the Ohkawa⁽⁹⁾ analytical expression for the distribution parameters, C_0 . For V_{gj} , RELAX uses a more detailed set of correlations whose magnitudes have been modified to be consistent with the Ohkawa

expression for C_0 . This approach has the advantage of using a consistent C_0 , V_{gj} set that is in agreement with flooding phenomena and the familiar Ishii⁽⁸⁾ correlations. Further, use of more refined correlations for V_{gj} together with a flow regime map allows a more detailed and better understanding of the flow conditions. In RELAX, Ohkawa's model is extended into co-current downward flow, inverted annular flow, and to both Wallis and Kutateladze flooding.

At high void fractions, flooding or annular flow tend to prevail. In flooding, the component volumetric fluxes (j_g , j_f) are computed by the flooding correlation independent of C_0 and V_{gj} . In annular flow, component volumetric fluxes are computed in terms of the mean transport drift velocity, \bar{V}_{gj} , which is transparent to the choice of C_0 . Thereby, at high void fractions, C_0 itself makes no significant contribution to the RELAX slip model. At lower void fractions, C_0 conforms to Ishii's⁽⁸⁾ latest correlations.

The dependence of V_{gj} on void fraction and mass flux is organized by a flow regime map. The flow regime map has regions of specified flow pattern and transition regions. The purpose of the transition regions is to smooth drift flux parameters at flow regime boundaries.

A variation of the flow regime map of the TRAC⁽¹⁶⁾ code is used in RELAX. TRAC uses a modification of the Bennett⁽¹⁷⁾ map for vertical flow. Figure 2.1 shows the RELAX flow regime map. The independent variables are total mass flux and void fraction. The effect of pressure and geometry are largely introduced by density and diametral dependence in the analytical correlations. Large volume-to-surface nodes (large hydraulic diameters) are restricted to the

churn-turbulent regions of the RELAX flow regime map; thereby, regimes dependent upon wall shear phenomena are avoided when the bulk of the coolant mass is far from the bounding walls.

2.2.1 Profile Slip, C_o

The distribution or profile slip parameter C_o has been introduced in Section 2.1. Here, the assignment of a numerical value to C_o based upon experimental results is discussed. RELAX uses the Ohkawa⁽⁹⁾ formulation for C_o . Ohkawa derives by synthesis a flooding compatible set of drift flux parameters for vapor phase flows in the upward direction. These equations are given by

$$C_o = \begin{cases} \min(C_{o1}, C_{o2}), & \text{for } \alpha \geq X \\ C_{o1}, & \text{for } \alpha < X \end{cases} \quad (2.5)$$

where

$$C_{o1} = [1.2 - 0.2 R] [1.0 - \text{EXP}(-18\alpha)]$$

$$C_{o2} = 1.0 + 0.2 [1.0 - R] [1.0 - \left(\frac{\alpha-X}{1-X}\right)^2]$$

$$R = (\rho_g/\rho_f)^{1/2}$$

$$X = 0.5881164 - 1.81701R + 2.00025R^2 - 3.34398R^3.$$

Figure 2.2 provides a plot of Equation 2.5 at 100 psia (0.7 Mpa).

2.2.2 Local Slip, V_{gj}

Referring to the lettered regions in the flow regime map shown in Figure 2.1, the following procedure is used to define V_{gj} . For bubble flow⁽¹¹⁾ (B: $0.01 \leq \alpha < 0.1$, $G \leq 2000 \text{ kg/m}^2\text{-s}$) and for the churn-turbulent bubbly flow⁽¹¹⁾ (C: $0.01 \leq \alpha \leq 0.85$, $G \geq 3000 \text{ kg/m}^2\text{-s}$)

$$V_{gj} = 2.9 \left(\frac{\sigma g \Delta \rho}{2 \rho_f} \right)^{1/4}; \quad (2.6)$$

and for slug flow⁽⁹⁾ (S: $0.2 \leq \alpha \leq 0.65$, $G \leq 2000 \text{ kg/m}^2\text{-s}$),

$$V_{gj} = 0.710 \left(\frac{g D \Delta \rho}{\rho_f} \right)^{1/2}. \quad (2.7)$$

For annular flow (A: $0.85 \leq \alpha \leq 1.0$, $G \leq 2000 \text{ kg/m}^2\text{-s}$), the equations of Ishii⁽⁸⁾ and Ishii, Chawla and Zuber⁽¹⁰⁾ are used. Their full constitutive equations for laminar and turbulent films are retained without simplification for high mass flux. The annular mean transport drift velocity for laminar film flow in RELAX is given by:

$$\bar{V}_{gj} = \frac{8\mu_f \alpha^2}{\rho_m D f_i \xi} \left\{ -1 + \left[1 + \frac{f_i D \rho_m^2 (1-\alpha) \xi}{4\mu_f \alpha^3 \rho_g} \left[v_m + \frac{\Delta \rho g D^2 (1-\alpha)^2}{48\mu_f} \right] \right]^{1/2} \right\} \quad (2.8)$$

where the sign on \bar{V}_{gj} is opposite the acceleration of gravity.

For a turbulent film flow, the relative motion of the phases determines the equation form. For counter-current flow

$$\bar{v}_{gj} = \frac{bv_m + [-av_m^2 + (a + b^2)c]^{1/2}}{(a + b^2)} \quad (2.9)$$

where

$$a = \frac{f_i \xi \rho_g}{0.005 \alpha \rho_f (1-\alpha)^2}$$

$$b = \frac{\alpha \rho_g}{\rho_m (1-\alpha)}$$

$$c = \frac{\Delta \rho g D (1-\alpha)}{0.015 \rho_f}$$

For co-current flow upward

$$\bar{v}_{gj} = \frac{-bv_m + [av_m^2 + (a-b^2)c]^{1/2}}{(a-b^2)} \quad (2.10)$$

For co-current flow downward

$$\bar{v}_{gj} = \frac{-bv_m + [av_m^2 - (a-b^2)c]^{1/2}}{(a-b^2)} \quad (2.11)$$

where the sign on \bar{v}_{gj} is the same as the acceleration of gravity.

For high void fractions ($\alpha > 0.85$) in the mass flux transition region, the annular ($G > 2000 \text{ kg/m}^2\text{-s}$) and churn-turbulent bubbly flows ($G < 3000 \text{ kg/m}^2\text{-s}$) are assumed to be a weighted mixture of the annular or bubbly flow regime and droplet flow.

Annular flow presumes a mist is present throughout. At the unity void fraction limit, the regime approaches pure droplet flow. The basis for this approach is the method employed by Ishii⁽⁸⁾ for annular mist flow. A function (E_d) representing the liquid fraction in droplets was developed which is defined:

$$E_d = \frac{A_{\text{drop}}}{A_{\text{drop}} + A_{\text{liq}}}$$

Further, a function

$$\frac{E_d(1-\alpha)}{\alpha + E_d(1-\alpha)} = \frac{A_{\text{drop}}}{A_{\text{vapor}} + A_{\text{drop}}}$$

is used to weight the droplet drift velocity. This weighting is required to go to zero at the boundaries of annular flow ($\alpha = 0.85$ and $\alpha = 1.00$). The droplet effect will reach a maximum between these limits. For the case of the annular/annular mist flow, the expression given by Ishii⁽⁸⁾ is used

$$\bar{V}_{gj} = (\bar{V}_{gj})_{\text{annular}} + \frac{E_d(1-\alpha)}{\alpha + E_d(1-\alpha)} * 2.9 \left(\frac{\sigma g_c \Delta p}{\rho_g} \right)^{\frac{1}{4}} \quad (2.12)$$

where the two terms are the annular film and the mist contributions, respectively. The annular component uses a product $(1-\alpha)*(1-E_d)$ in place of $(1-\alpha)$ in order to consider only the effect of the film. The droplet contribution then describes the motion of droplet relative to the annular core.

The other transition regions in the flow regime map use linear weighting after the methods of the TRAC code⁽¹⁶⁾. This smooths all flow domain transitions. For the low quality domain (L: $\alpha < 0.01$, linear weighting to $V_{gj} = 0.0$ at $\alpha = 0.005$ is used. For lower void fractions ($0.0 \leq \alpha \leq 0.005$, all G), $V_{gj} = 0.0$.

fraction is shown for a range of mass fluxes within and near counter-current conditions. Flooding limits influence upflow in the higher void fraction range. This will be discussed in the next section.

2.3 CONSISTENCY WITH CCFL RELATIONS

The drift velocity, V_{gj} , used in RELAX is derived from first principles, as in annular flow, or has been determined from experimental results. These relations were summarized in the previous sections. Experiment has identified a limit of operation in counter-current flow which is known as the "flooding limit". For a given upward gas velocity, the flooding limit line yields the maximum downward liquid flow. Thereby, flooding places a limit on the drift velocity. RELAX permits the use of either a Wallis formulation⁽²²⁾, a Kutateladze formulation, or a combination as suggested by Lier and Collier⁽¹⁸⁾.

Either Wallis or Kutateladze flooding conditions^(5,9) (user selected) may be used as the basis for deriving a consistent C_o and V_{gj} at the flooding limit. RELAX uses this value as an upper limit for the liquid flux. Also as proposed by Kelly, et al⁽⁵⁾, this limit is used as a means of extending the drift velocity which is valid for lower void fractions to high void fractions.

For the Wallis flooding correlation

$$(j_g^*)^{1/2} + m (j_f^*)^{1/2} = C \quad (2.13)$$

where

$$j_g^* = [\rho_g j_g^2 / g^D \Delta \rho]^{1/2}$$

$$j_f^* = [\rho_f j_f^2 / g^D \Delta \rho]^{1/2}$$

Kelly, et.al.⁽⁵⁾ found the drift velocity at the flooding limit may be defined by

$$V_{gj}^F = \frac{V_{gc} C_o (1 - \alpha C_o)}{\alpha C_o + m^2 \left(\frac{\rho_f}{\rho_g}\right)^{1/2} (1 - \alpha C_o)} \quad (2.14)$$

This relation involves the flooding parameter, V_{gc} , where

$$V_{gc} = C^2 \left[\frac{\Delta \rho g^D}{\rho_g} \right]^{1/4} \quad (2.15)$$

The flooding coefficients m and C of Equation 2.13 appear in Equations 2.14 and 2.15, respectively. This derivation extends the tangent to the flooding curve into the co-current flow domains. This same tangent is line is obtained from the Zuber-Findlay equation.

For the Kutateladze flooding correlation

$$(K_g)^{1/2} + m (K_f)^{1/2} = C \quad (2.16)$$

where

$$K_g = [\rho_g j_g^2 / g g_c \sigma (\Delta \rho)]^{1/2 \cdot 1/2}$$

$$K_f = [\rho_f j_f^2 / g g_c \sigma (\Delta \rho)]^{1/2 \cdot 1/2}$$

is used, then V_{gj}^F may be shown to be unchanged, but

$$V_{gc} = C^2 \left[\frac{[gg_c \sigma \Delta \rho]^{1/2}}{\rho_g} \right]^{1/2} \quad (2.17)$$

For upward directed gas flow, the drift velocity is computed as follows:

$$V_{gj} = \text{minimum} (V_{gj}^F, V_{gj}^P) \quad (2.18)$$

where V_{gj}^P is the value based solely on consideration of the flow pattern (Figure 2.1). For a mass flux directed downward in co-current flow, the flooding limit is not required and is not used.

The above procedure amounts to the projection of the surface in the $j_f-j_g-\alpha$ system defined by the Zuber-Findlay equation onto the j_f-j_g plane. This projection defines the flooding line. A typical plot of the Zuber-Findlay equation predictions using drift flux parameters (V_{gj} , C_o) based upon flow regime (see Section 2.2) is shown in Figure 2.4. Also plotted is the Kutateladze flooding limit correlation. Consistency of the Zuber-Findlay surface projection and the flooding line is illustrated.

2.4 VOID FRACTION SELECTION

The drift flux parameters V_{gj} and C_o discussed in the previous section are functions of the void fraction. The void fraction used in the RELAX drift flux calculations is computed from conditions on either side of the RELAX junction. For co-current flow, the code permits the user to

specify a weighted average of homogeneous void fractions in the donor and receiver cells. Recommended weighting is heavily towards the donor volume (between 80% and 100% donor). The latter (100%) is particularly recommended where phase separation volumes are also used.

For counter-current flow, the void fraction is based upon the assumption of junction flooding when sufficient liquid exists at the junction for flooding to occur. Thus, for a net mass flux the volumetric fluxes, j_g and j_f , are established independent of the void fraction. The solution is found at the intersection of the flooding correlation (Equations 2.13 or 2.16) and the mass continuity equation (Equation 2.4) as shown in Figure 2.5 (point A). The void fraction is then obtained by equating the slope of the flooding correlation to the slope of the Zuber-Findlay equation at flooding point as

$$\left(\frac{j_f}{j_g} \right)^{1/2} = m \left(\frac{\rho_f}{\rho_g} \right)^{1/4} \left(\frac{1 - C_0 \alpha^F}{C_0 \alpha^F} \right)$$

The void fraction, α^F , is solved by iteration where $C_0 = C_0(\alpha)$. If α^F is bracketed between the void fractions of the adjacent volumes, it becomes the counter-current void fraction. If α^F is not within this range, the void fraction is based on the liquid flow from within the upper volume and the vapor flow from within the lower volume.

2.5 DRIFT FLUX MODEL IMPLEMENTATION

The RELAX blowdown code is derived from RELAP4 version ENC28B⁽¹⁾.

The following section describes how the drift flux model has been interfaced with the RELAP4 type flow solution. RELAX considers a network of control volumes and flow junctions with homogeneous flow. The drift flux model is applied to user designated junctions. Drift flux is applicable only to junctions having an elevation change (vertical flow) when two-phase flow exists.

The dominant effect of slip flow is in the convective energy term in the total energy equation. In RELAX, enthalpy transfer is based upon the individual vapor and liquid flows. Homogeneous flow, as in RELAP4/ENC28B, computes the equivalent term based upon total mixture flow (liquid and vapor velocities equal). Thus, RELAX allows the calculation of more realistic energy convection for vertical two-phase flows when slip flow (drift flux) is specified at a junction.

2.5.1 Basic Equations of Motion

The basic conservation equations of motion of RELAX are identical to the integrated stream-tube fluid equations of RELAP4^(20,21) except the energy equation has been refined.

The RELAP4 homogeneous flow energy equation is

$$\frac{dU_i}{dt} = -\frac{\ell_i}{2A_i} \frac{d}{dt} \left(\frac{\bar{W}_i^2}{\rho_i} \right) + \sum_j W_j \left(h_j + \frac{V_j^2}{2} + z_j - z_i \right) + Q_i .$$

The RELAX program redefines the convective energy transfer term so that the energy equation becomes

$$\frac{dU_i}{dt} = -\frac{\ell_i}{2A_i} \frac{d}{dt} \left(\frac{\bar{W}_i^2}{\rho_i} \right) + \sum_j W_{\ell j} h_{\ell j} + \sum_j W_{g j} h_{g j} + \sum_j W_j \left(\frac{V_j^2}{2} + z_j - z_i \right) . \quad (2.19)$$

The average mass flow in volume \bar{W}_i (usually written hereafter as W) as used in Equation 2.19 is defined in RELAX as

$$\bar{W}_i = \frac{\sum_{in} W_j - \sum_{out} W_j}{2} \quad (2.20)$$

2.5.2 Difference Equations with Drift Flux

The differential equations in RELAX may be written with time level (n) notation

$$\begin{aligned} \frac{dU}{dt} &= \theta f_1^{n+1} + (1-\theta)f_1^n + f_2^n \\ \frac{dM}{dt} &= \theta g_1^{n+1} + (1-\theta)g_1^n + g_2^n \\ \frac{dW}{dt} &= \theta q_1^{n+1} + (1-\theta)q_1^n + q_2^n \end{aligned} \quad (2.21)$$

where the functional notation is in terms of the independent variables U, M, W, t . The component parts of the energy equation will be focused on since only the energy equation is altered by drift flux. These are

$$\begin{aligned} f_1^{n+1} &= \sum_{in} W_j^{n+1} e_j^n - \sum_{out} W_j^{n+1} e_j^n, \\ f_2^n &= -\frac{\ell_i}{2A_i} \frac{d}{dt} \left(\frac{\bar{W}_i^2}{\rho_i} \right) + Q_i \end{aligned} \quad (2.22)$$

where

$$W_j^{n+1} e_j^n = W_{g_j}^{n+1} h_{g_j}^n + W_{f_j}^{n+1} h_{f_j}^n + W_j^{n+1} \left[\frac{(v_j^n)^2}{2} + z_j - z_i \right] \quad (2.23)$$

The energy equation may be simplified further:

$$\frac{dU}{dt} = \theta f_1^{n+1} - \theta f_1^n + F^n, \quad \text{where } F^n = f_1^n + f_2^n.$$

When linearized using a first order accurate forward finite difference approximation, one obtains

$$\Delta U = r^n \Delta t + \left[\Delta U \left(\frac{\partial f_1}{\partial U} \right)_{M,W}^n + \Delta M \left(\frac{\partial f_1}{\partial M} \right)_{U,W}^n + \Delta W \left(\frac{\partial f_1}{\partial W} \right)_{U,M}^n \right] \Delta t \theta. \quad (2.24)$$

This and companion equations for mass and flow increments are common to both the homogeneous and drift flux flows. The coefficient θ is the Crank Nicholson implicit-explicit multiplier. When $\theta = 0$ the equation will be fully explicit, and when $\theta = 1$ the equation will be fully implicit. This input parameter is normally fixed at unity. Consider the derivatives of Equation 2.24 that make up the terms of the Jacobian (terms in large brackets):

$$\left(\frac{\partial f_1}{\partial U}\right)_{M,W}^n \Delta U = 0$$

$$\left(\frac{\partial f_1}{\partial M}\right)_{U,W}^n \Delta M = 0$$

$$\left(\frac{\partial f_1}{\partial W}\right)_{U,M}^n \Delta W = \frac{\partial}{\partial W} \left(\sum_{in} W_j^n e_j^n \Delta W_j \right) - \frac{\partial}{\partial W} \left(\sum_{out} W_j^n e_j^n \Delta W_j \right)$$

The individual component contributions to kinetic and potential energy are ignored, so a typical term in F^n is

$$\sum_{in} (W_j^n e_j^n) = \sum_{in} \left(W_{g_j}^n h_{g_j}^n + W_{\ell_j}^n h_{\ell_j}^n + W_j^n \left(\frac{(v_j^n)^2}{2} + z_j - z_i \right) \right) \quad (2.25)$$

The Jacobian in Equation (2.24) follows a similar approach

$$\begin{aligned} \frac{\partial}{\partial W} \sum_{in} (W_j^n e_j^n W_j) &= \sum_{in} \frac{\partial}{\partial W_g} (W_j^n e_j^n) \frac{\partial W_g}{\partial W} \Delta W_j \\ &+ \sum_{in} \frac{\partial}{\partial W_\ell} (W_j^n e_j^n) \frac{\partial W_\ell}{\partial W} \Delta W_j \end{aligned} \quad (2.26)$$

The derivatives $\partial W_g / \partial W$ and $\partial W_\ell / \partial W$ are needed to evaluate 2.26 and may be computed from the expression

$$j_g = \alpha (j + \bar{v}_{gj}).$$

One obtains from differentiation

$$\frac{\partial W_\ell}{\partial W} = \frac{(1-\alpha)\rho_\ell}{\rho} - \alpha\rho_g A \frac{\partial \bar{V}_{gj}}{\partial W}, \text{ and } \frac{\partial W_g}{\partial W} = \frac{\alpha\rho_g}{\rho} + \alpha\rho_g A \frac{\partial \bar{V}_{gj}}{\partial W}.$$

Thereby, Equations 2.25 and 2.26 lead to

$$\begin{aligned} \frac{\partial}{\partial W} \left(\sum_{in} W_j^n e_j^n \Delta W_j^n \right) &= \sum_{in} (h_{gj}^n \left[\frac{\alpha\rho_g}{\rho} + \alpha\rho_g A \frac{\partial \bar{V}_{gj}}{\partial W} \right] \\ &+ h_{\ell j}^n \left[\frac{(1-\alpha)\rho_\ell}{\rho} - \alpha\rho_g A \frac{\partial \bar{V}_{gj}}{\partial W} \right] + \left(\frac{V_j^n}{2} + z_j - z_i \right) \Delta W_j. \end{aligned}$$

Thus, Equation 2.26 becomes

$$\begin{aligned} \Delta U_i - \theta \Delta t \left(\sum_{in} (h_{gj}^n \left[\frac{\alpha\rho_g}{\rho} + \alpha\rho_g A \frac{\partial \bar{V}_{gj}}{\partial W} \right] + h_{\ell j}^n \left[\frac{(1-\alpha)\rho_\ell}{\rho} - \alpha\rho_g A \frac{\partial \bar{V}_{gj}}{\partial W} \right] \right. \\ \left. + \frac{(V_j^n)^2}{2} + z_j - z_i \right) \Delta W_j \\ - \left(\sum_{out} (h_{gj}^n \left[\frac{\alpha\rho_g}{\rho} + \alpha\rho_g A \frac{\partial \bar{V}_{gj}}{\partial W} \right] + h_{\ell j}^n \left[\frac{(1-\alpha)\rho_\ell}{\rho} - \alpha\rho_g A \frac{\partial \bar{V}_{gj}}{\partial W} \right] \right. \\ \left. + \frac{(V_j^n)^2}{2} + z_j - z_i \right) \Delta W_j \Big) = F_i^n \Delta t \theta \end{aligned} \quad (2.27)$$

where properties ρ , ρ_g , ρ_ℓ , α and A are evaluated at the junction of interest at time n and

where

$$\begin{aligned}
 F_i^n &= \sum_{\text{in}} \left(W_{g_j}^n h_{g_j}^n + W_{l_j}^n h_{l_j}^n + W_j^n \left(\frac{(V_j^n)^2}{2} + z_j - z_i \right) \right) \\
 &\quad - \sum_{\text{out}} \left(W_{g_j}^n h_{g_j}^n + W_{l_j}^n h_{l_j}^n + W_j^n \left(\frac{(V_j^n)^2}{2} + z_j - z_i \right) \right) \\
 &\quad - \frac{\ell_i}{2A_i} \frac{d}{dt} \frac{\bar{W}_i^2}{\rho_i} + Q_i.
 \end{aligned} \tag{2.28}$$

Drift flux modifications to the energy equation are made in both the Jacobian (see major bracketed term in Equation 2.27) and the right-hand side vector (Equation 2.28). In the absence of drift flux, the energy equation reverts to a homogeneous flow characterization: (1) the coefficients of ΔW_j in Equation 2.27 become

$$\left(h_j^n + \frac{(V_j^n)^2}{2} + z_j - z_i \right)$$

and (2) the convective energy terms in Equation 2.28 become

$$\left(W_j^n \left[h_j^n + \frac{(V_j^n)^2}{2} + z_j - z_i \right] \right)$$

2.5.3 Anatomy of Drift Flux Model in Code

The drift flux model is implemented in RELAX by the introduction of four new subroutines. These are

NEWSLP - Controls drift flux calculations. Calculates superficial component fluxes and flow rates.

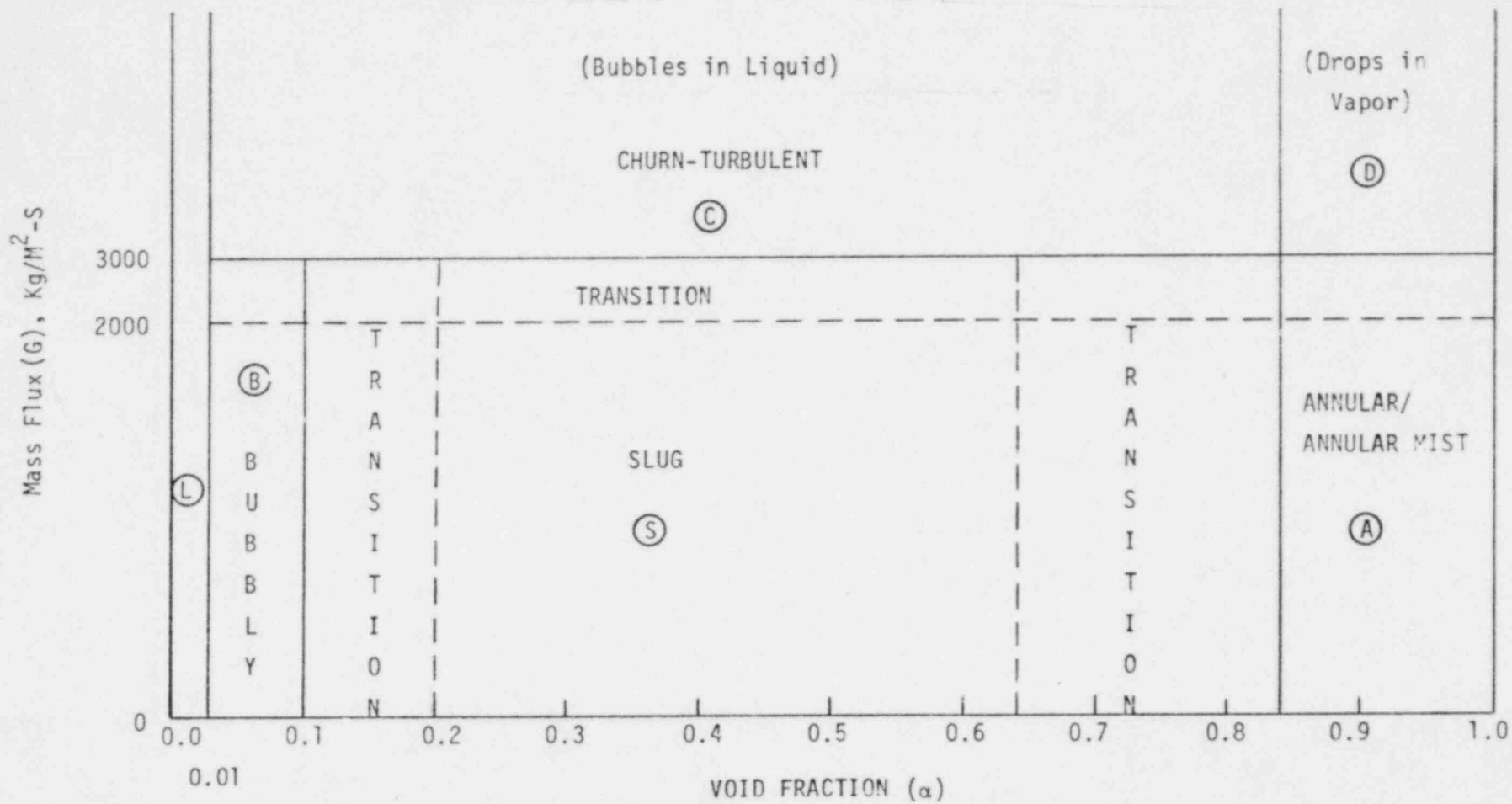
DRIFT - Determines V_{gj} and C_o as a function of location on flow regime map.

ANULAR - Determines \bar{V}_{gj} for annular flow.

CCFLOW - Determines α , V_{gj} and C_0 for flooded counter-current flow.

The key to success of the drift flux model in RELAX is the reduction of thermal hydraulic discontinuities. Excessively rapid changes in flow rate, density, pressure, etc. have been avoided by the smoothing of the drift flux parameters of the flow regime transition and by avoiding rapid changes in time step size.

Figure 2.1 RELAX FLOW REGIME MAP FOR DRIFT FLUX CORRELATIONS



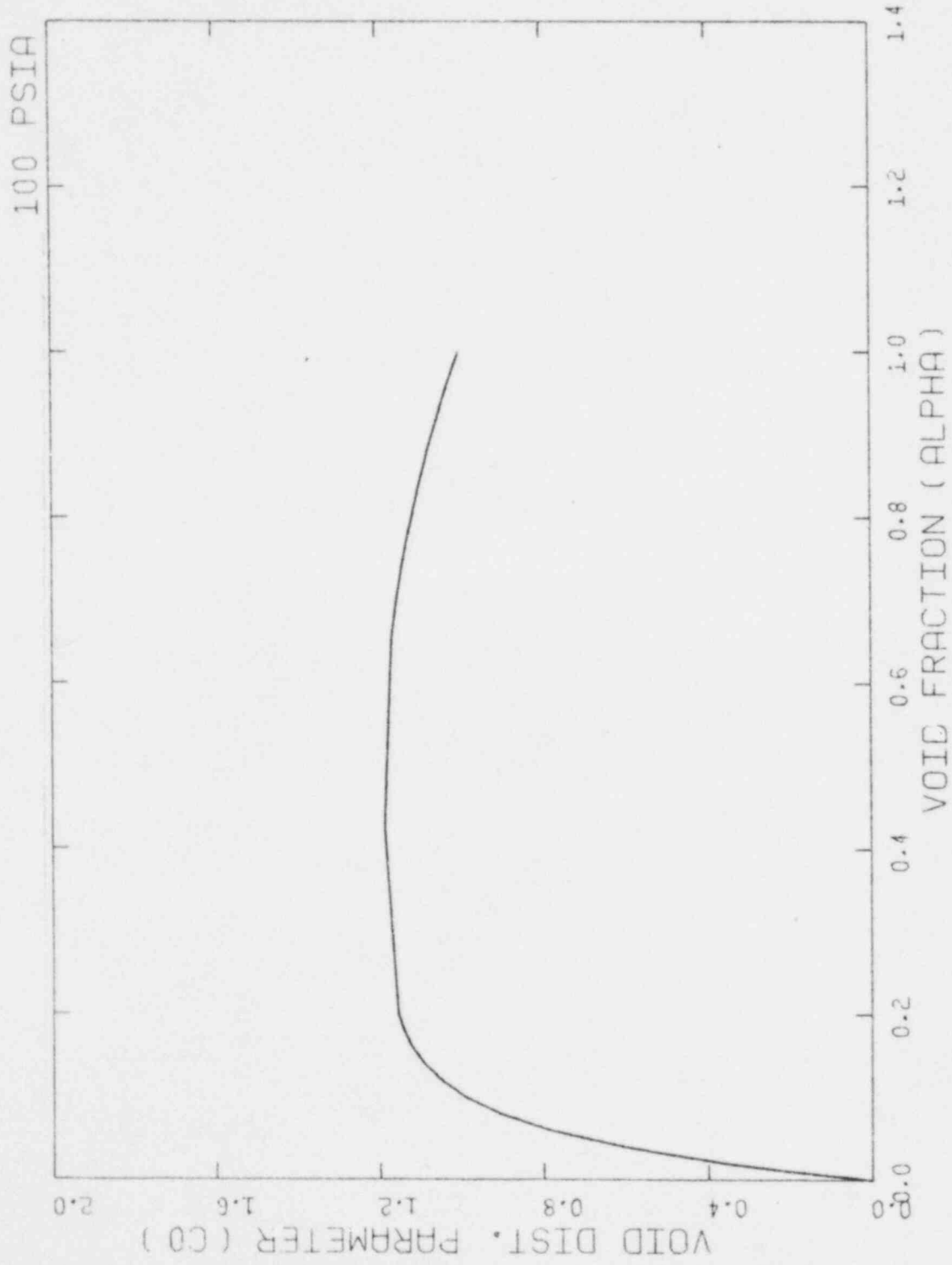


Figure 2.2 Distribution Parameter predicted by RELAX at 100 psia

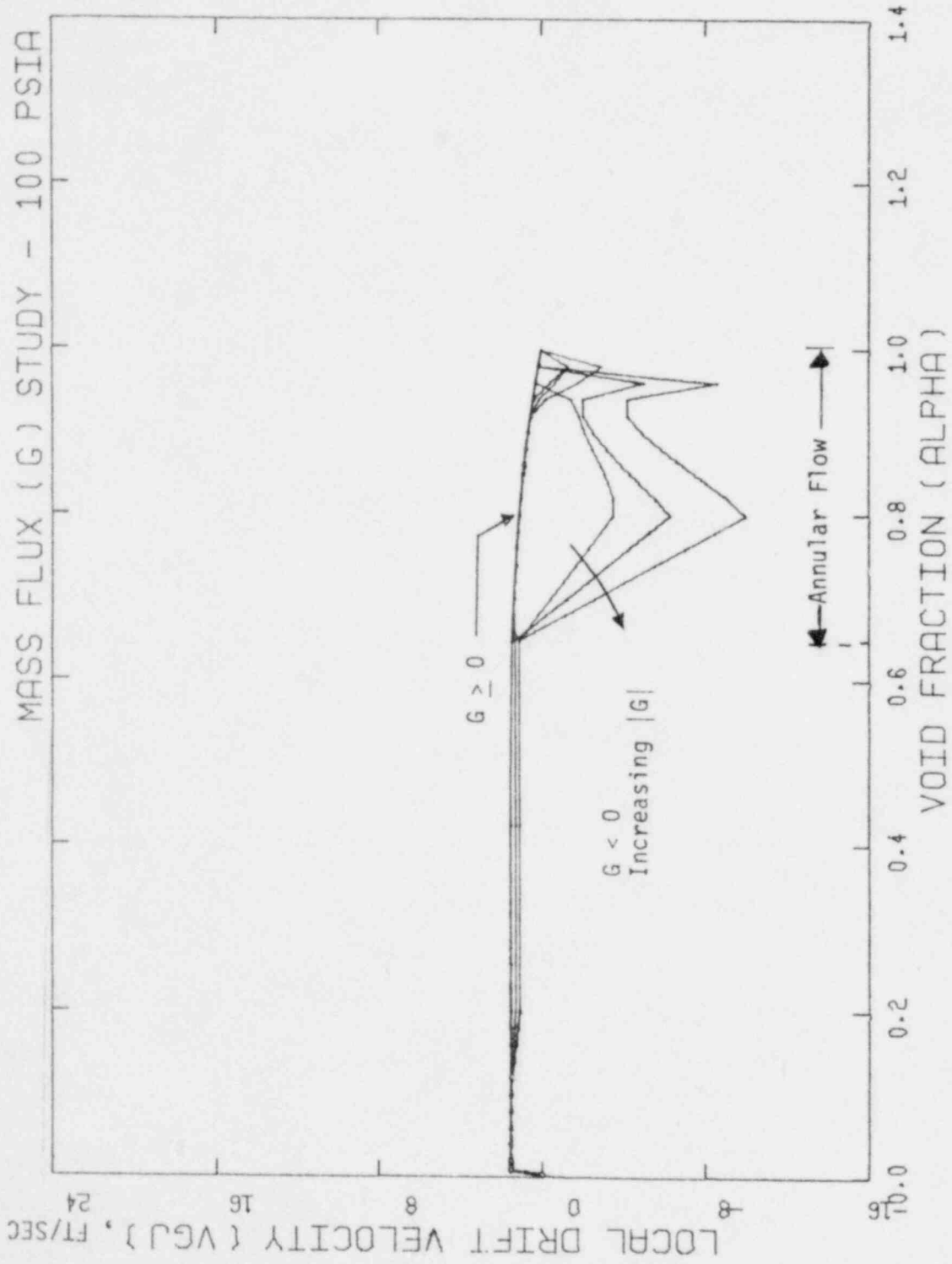


Figure 2.3 Local Drift Velocity versus Void Fraction
at 100 psia

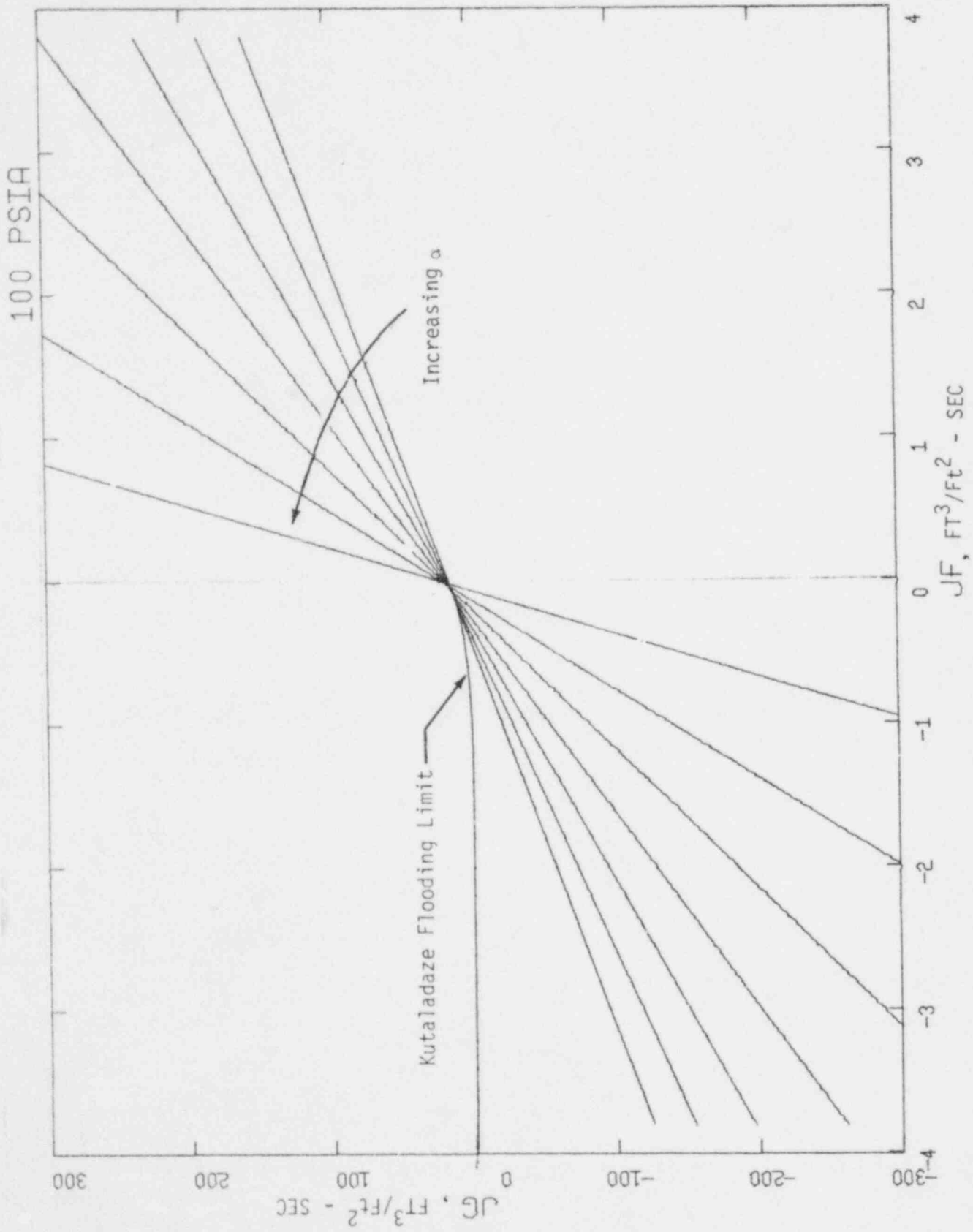


Figure 2.4 Gas versus Liquid Volumetric Fluxes from Zuber-Findlay Equation at 100 psia

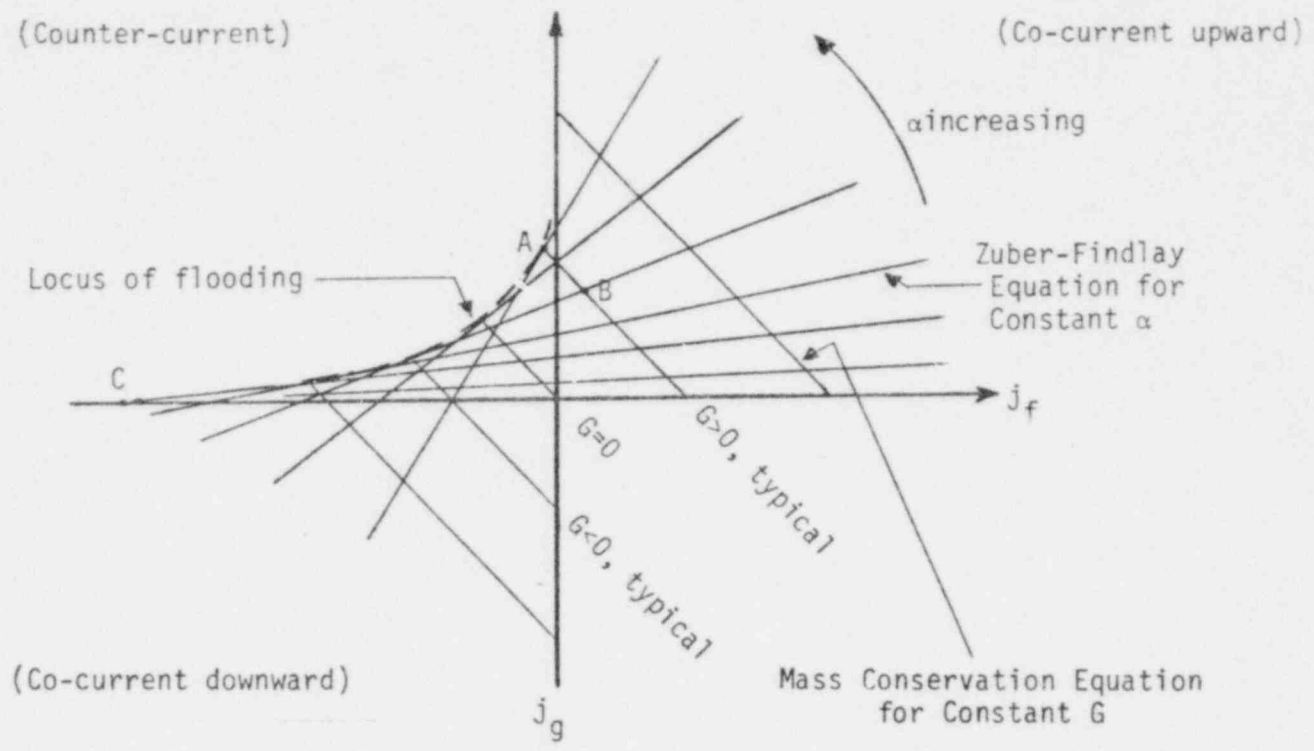


Figure 2.5 TWO-DIMENSIONAL j_g - j_f PLANE

3.0 JET PUMP MODEL

This section describes the model used to simulate jet pumps in the RELAX code. A mechanistic model is used in order to include the effects of scale (size) and various design features. The two-dimensional equations of fluid motion are solved

These equations are solved numerically in a side calculation to obtain the jet pump pressure change due to momentum mixing and friction. This pressure change is combined with the volume-wide jet pump pressure loss. The result is then introduced into the RELAX general solution scheme just as it is in RELAP4. Empiricism is introduced by one set of friction and pressure loss coefficients.

The jet pump model includes flow momentum interactions for all possible flow combinations. To describe the basic flow patterns which might exist in the jet pump, it is useful to consider the M-N performance curve shown in Figure 3.1. The dimensionless flow parameter M is defined as the ratio of suction (s) and drive (d) flow rates

$$M = \frac{W_s}{W_d} \quad (3.1)$$

and the pressure drop parameter is defined as the ratio of total pressure differences given by

$$N = \frac{p_e^* - p_s^*}{p_d^* - p_e^*} \quad (3.2)$$

The six possible flow combinations are illustrated in Figure 3.1. The forward drive and forward suction flow combination (type 1+) is the normal operation condition.

3.1 JET PUMP NODING

The nodalization used to model a jet pump in RELAX is consistent with the conventional modeling in RELAP4. Figure 3.2 shows a schematic of a jet pump and the equivalent system nodal modeling used in RELAX. The system is modeled with a volume for the drive, suction and jet pump. A pair of junctions connect the drive and suction volumes to the common jet pump volume. Up to this point, the modeling is the same as in RELAP4.

The modeling departure for RELAX occurs in the jet pump momentum mixing section.

The mixing section is not apparent to the user of RELAX and may not be changed by the input except for overall mixing section dimensions. The mixing section dimensions and volume serve only to aid the calculation of the pressure drop in the drive and suction junctions of the jet pump. It has no volume in the RELAX code since its volume is assigned to the jet pump volume as shown in Figure 3.2.

3.2 STREAM TUBE MODELING

As with RELAP4, the jet pump model description is based on a composite two-stream one-dimensional momentum equation. Flow solutions for each of the jet pump input streams are coupled through the mixing region model. Section 3.3 will describe the theory within the jet pump mininode mixing region. This section describes the overall integration of the mininode mixing region model results into RELAX.

Consider the schematic picture of the BWR jet pump in Figure 3.4. Variables for flow and pressure have been identified for drive, suction and jet pump volumes, and the boundaries at the jet pump mixing junction. The pressures P_K , P_M , and P_L and the flows \bar{W}_K , \bar{W}_M , and \bar{W}_L are assumed to be at the center of RELAX volumes. The pressure P_D is assumed to be in the drive volume just ahead of the drive nozzle. The pressure P_S is in the suction volume just ahead of the suction inlet. The pressure P_E is at the end of the mixing section.

The philosophy of the new jet pump model is to compute the pressure differences $P_e - P_d$ and $P_e - P_s$ for the mixing region such that the integration of the RELAX flow momentum equations can be done for K to L and M to L.

The one-dimensional stream-tube flow momentum equation which forms the basis for RELAX can be written as:

$$\frac{1}{A} \frac{\partial W}{\partial t} + \frac{1}{A} \frac{\partial UW}{\partial x} + \frac{\partial P}{\partial x} = - \frac{1}{A} \frac{\partial F}{\partial x} - \rho g \quad (3.3)$$

The integration of Equation 3.3 along the suction (M-S-s), drive (K-D-d) and diffuser (e-E-L) streams follows standard RELAX (or RELAP4) procedures^(12,20). Integration through the mixing region (s-e and d-e) is done to obtain the pressure differences ($P_e - P_s$) and ($P_e - P_d$). These pressure differences, ΔP_{de} and ΔP_{se} for the drive and suction parts of the mixing section as defined as

$$-\Delta P_{de} = \left(P + \left(\frac{UW}{A} \right) + H \right)_e - \left(P + \left(\frac{UW}{A} \right) + H \right)_d, \quad (3.4)$$

$$-\Delta P_{se} = \left(P + \left(\frac{UW}{A} \right) + H \right)_e - \left(P + \left(\frac{UW}{A} \right) + H \right)_s. \quad (3.5)$$

The complete equation for the drive junction is the sum of all components along the path K-D-d-e-E-L. The result is given below in terms of the inertia ($I_i = L_i/A_i$):

$$\begin{aligned} \frac{1}{2} (I_K + I_L) \frac{\partial W_D}{\partial t} &= (P + \left(\frac{\bar{W}}{A} \right)^2 v + H)_K - (P + \left(\frac{\bar{W}}{A} \right)^2 v + H)_L \\ &- \frac{1}{2} \left(\frac{fL_v}{2D} \frac{|\bar{W}|\bar{W}}{A} \right)_{KD} - \frac{1}{2} \left(\frac{fL_v}{2D} \frac{|\bar{W}|\bar{W}}{A^2} \right)_{EL} - \frac{I_L}{2} \frac{\partial W_S}{\partial t} \\ -\Delta P_{de} & \end{aligned} \quad (3.6)$$

The heights H_d , H_D , H_e and H_E are taken to be equal.

Similarly, for the suction

$$\begin{aligned} \frac{1}{2} (I_M + I_L) \frac{\partial W_S}{\partial t} &= (P + \left(\frac{\bar{W}}{A} \right)^2 v + H)_M - (P + \left(\frac{\bar{W}}{A} \right)^2 v + H)_L \\ &- \frac{1}{2} \left(\frac{fL_v}{2D} \frac{|\bar{W}|\bar{W}}{A^2} \right)_{MS} - \frac{1}{2} \left(\frac{fL_v}{2D} \frac{|\bar{W}|\bar{W}}{A^2} \right)_{EL} - \frac{I_L}{2} \frac{\partial W_D}{\partial t} \\ -\Delta P_{se} & \end{aligned} \quad (3.7)$$

The following section describes how the terms ΔP_{de} and ΔP_{se} are determined through the mixing model.

3.3 MIXING REGION EQUATIONS

The previous section presented the integration of the stream tube equations outside of the jet pump mixing region. This section presents the equations inside the mixing region as applied to the mininodalization of Figure 3.3. This solution is used to couple the stream tube equations by determining ΔP_{de} and ΔP_{se} .

The principal assumptions used to develop the equations are as follows:

1)

2)

3) Choking within the jet pump is considered by taking the minimum of the flow momentum solution or the approved evaluation model correlation(s) for critical flow.

- 4) The mixing section is considered to have volume for purposes of defining the pressure drop effect of flow momentum mixing. However, it is assumed to have no thermodynamic volume. The mixing region is assumed to occupy only the junction interface between the drive, suction and jet pump volumes. This is consistent with previous modeling in RELAP4. The jet pump volume is fully accounted for by standard RELAX volume modeling (see Figure 3.2).
- 5) The mixing region pressure drop is defined on the basis of steady-state flow. This is consistent with assumption 4.
- 6)

The jet pump model equations are derived for the mixing section by using steady mass and momentum balance equations. Transient terms are retained as a convenience for the iteration process.

The continuity equation is expressed in a convective form:

$$\frac{\partial \rho U}{\partial x} + \frac{\partial \rho V}{\partial y} = 0 \quad (3.8)$$

The momentum equations are as follows:

$$\rho \frac{\partial U}{\partial t} = - \left(\rho U \frac{\partial U}{\partial x} + \rho V \frac{\partial U}{\partial y} \right) - \frac{\partial P}{\partial x} - F_x \quad (3.9)$$

$$\rho \frac{\partial V}{\partial t} = - \rho U \frac{\partial V}{\partial x} - \frac{\partial P}{\partial y} \quad (3.10)$$

A representative example of the jet pump momentum equation set is provided below. Boundary conditions are known

The axial momentum equation (3.9) for the drive side

(3.11)

and for the suction side is:

(3.12)

The fluid-to-fluid shear force is written as

$$(3.13)$$

and the wall shear force is

$$(3.14)$$

The lateral momentum equation (3.10) is also required to couple the transverse pressure and the cross flow . It is written in finite difference form for Section B and the last half of Section C in conservation form

(3.22)

(3.23)

(3.24)

These momentum equations are solved together with similar momentum equations and the continuity equation (3.10) for the desired mixing volume pressure drops (ΔP_{de} and ΔP_{se}).

The drive junction jet diameter flow area (A_d) is adjusted for small expansions and contractions in the mixing region by the following empirically based (data of Reference 24) expression:

3.4 NUMERICAL SOLUTION

The mass and momentum equations (Equations 3.8, 3.9 and 3.10) are solved simultaneously for steady-state by using a transient solution algorithm. This is done for convenience since the selected transient solution procedure provides a fast route to a steady-state solution. The solution approach is based on the ICE algorithm developed at Los Alamos Scientific Laboratory⁽²³⁾. The algorithm uses a predictor-corrector strategy to advance the solution through successive time steps.

A summary of the solution procedure is as follows:

3.5 IMPLEMENTATION OF JET PUMP MODEL IN RELAX

The jet pump model was primarily implemented in RELAX by providing an additional option in Subroutine MIXFLO. That option calls subroutine JETPMF rather than executing the previous existing momentum mixing options in MIXFLO. Other minor changes were required in subroutines PREW and INJUN to accommodate the new option.

3.6 RELAX MODELING IN VICINITY OF JET PUMP

This section discusses how the user models the drive, downcomer and jet pump mixer/diffuser volumes in RELAX.

The jet pump drive (or the selected portion of the drive) is modeled as a single volume in RELAX. The model volume preserves: 1) the actual volume of the fluid in the drive line and nozzle; 2) the flow area of the drive line; 3) the length of the drive line; and 4) the equivalent hydraulic diameter of

the drive line. The junction area from the drive line to the mixing section is the minimum flow area of the drive nozzle.

The jet pump suction volume is modeled as a single volume and may be connected to several jet pumps. The fluid volume is the volume outside the jet pump in the downcomer. The volume flow area is the downward projected area of the downcomer without the jet pump. The length for inertia is the distance from the top of the jet pump suction to the top of the downcomer volume. The equivalent hydraulic diameter is based upon the standard definition of four times the flow area divided by the wetted perimeter. The suction junction flow area is input as the flow area of the mixing section minus the flow area of the drive junction.

The momentum mixing section of the jet pump is modeled as a "massless" volume for the purpose of defining the pressure difference between the jet pump and the drive and suction. The actual mixing section geometry, however, is used to calculate the pressure difference. Input required for the jet pump model are the mixing section flow area, length, diameter, the drive jet diameter, forward and reverse loss coefficients and shear loss coefficients.

The jet pump is modeled as a single volume. The volume consists of the individual volumes of mixing section, diffuser and exit pipe as shown in Figure 3.2. Specification of jet pump volume, length and area is straightforward. The equivalent hydraulic diameter is modeled to give the same friction pressure drop as in the actual pump.

Multiple jet pumps can be modeled as single jet pumps. This is accomplished by multiplying the area, volume and flow of the individual pumps

by the number of pumps. The hydraulic diameter for the composite pump is the same as for any individual pump that is represented. This assures the same pressure drop for the composite jet pump as the single jet pump.

3.7 LOSS COEFFICIENTS

Four forward and reverse pressure loss coefficients and two wall shear coefficients are used in the jet pump mixing region. These coefficients are introduced as code input.

The pressure coefficients recommended for the drive and suction are illustrated in Figure 3.6. The shear coefficients ($C_T = f/4$) recommended between the fluid streams and the wall are:

Fluid-fluid shear -

Wall shear -

The basis for these recommendations are the extensive 1/6 scale tests conducted by EG&G⁽²⁴⁾ as well as full size jet pump data. Figure 3.7 provides a comparison between experimental data and calculated curves in M-N space for EG&G jet pump tests.

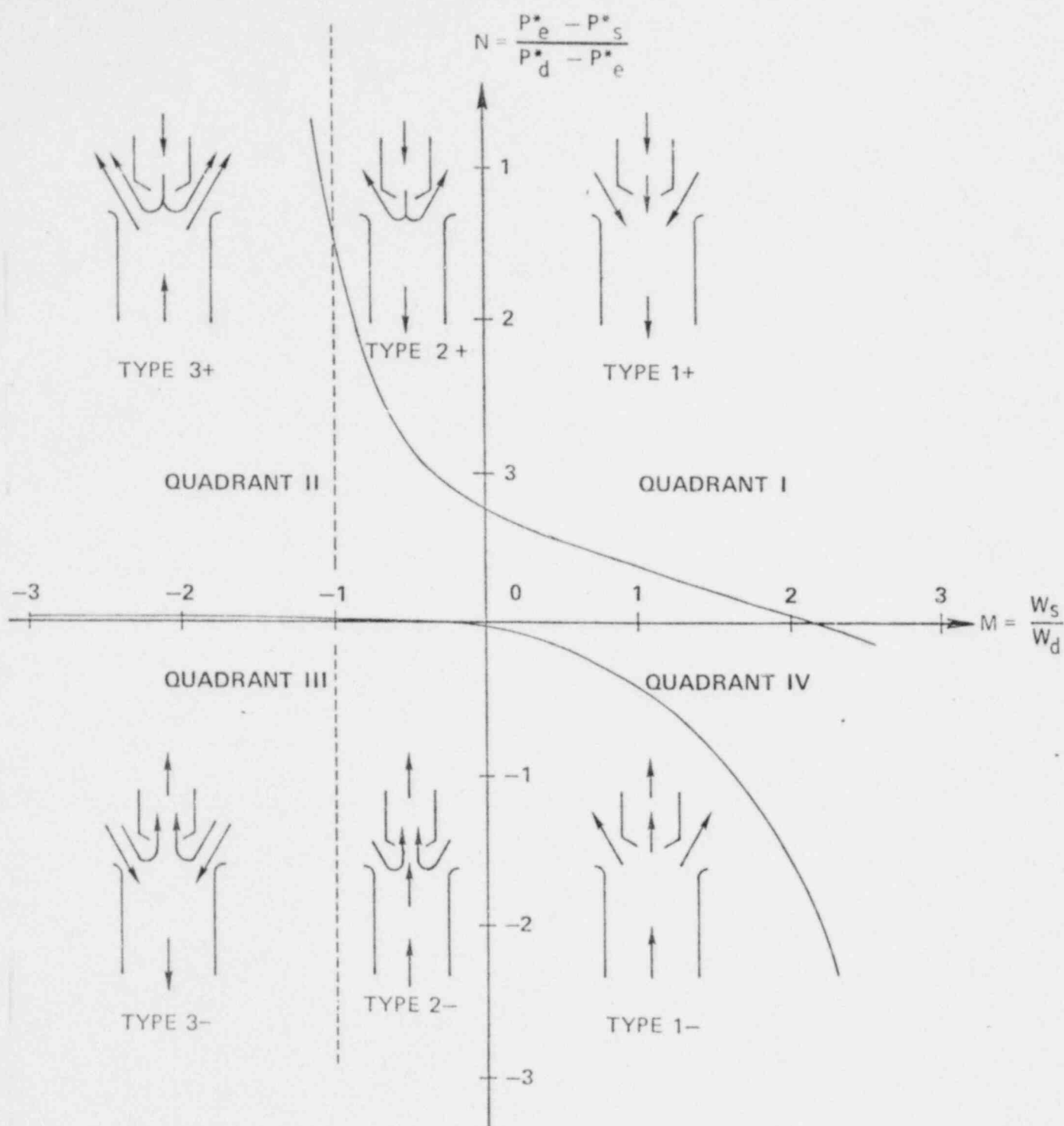


FIGURE 3-1 TYPICAL N-M JET PUMP CURVE WITH CLASSIFICATION OF FLOW TYPES.

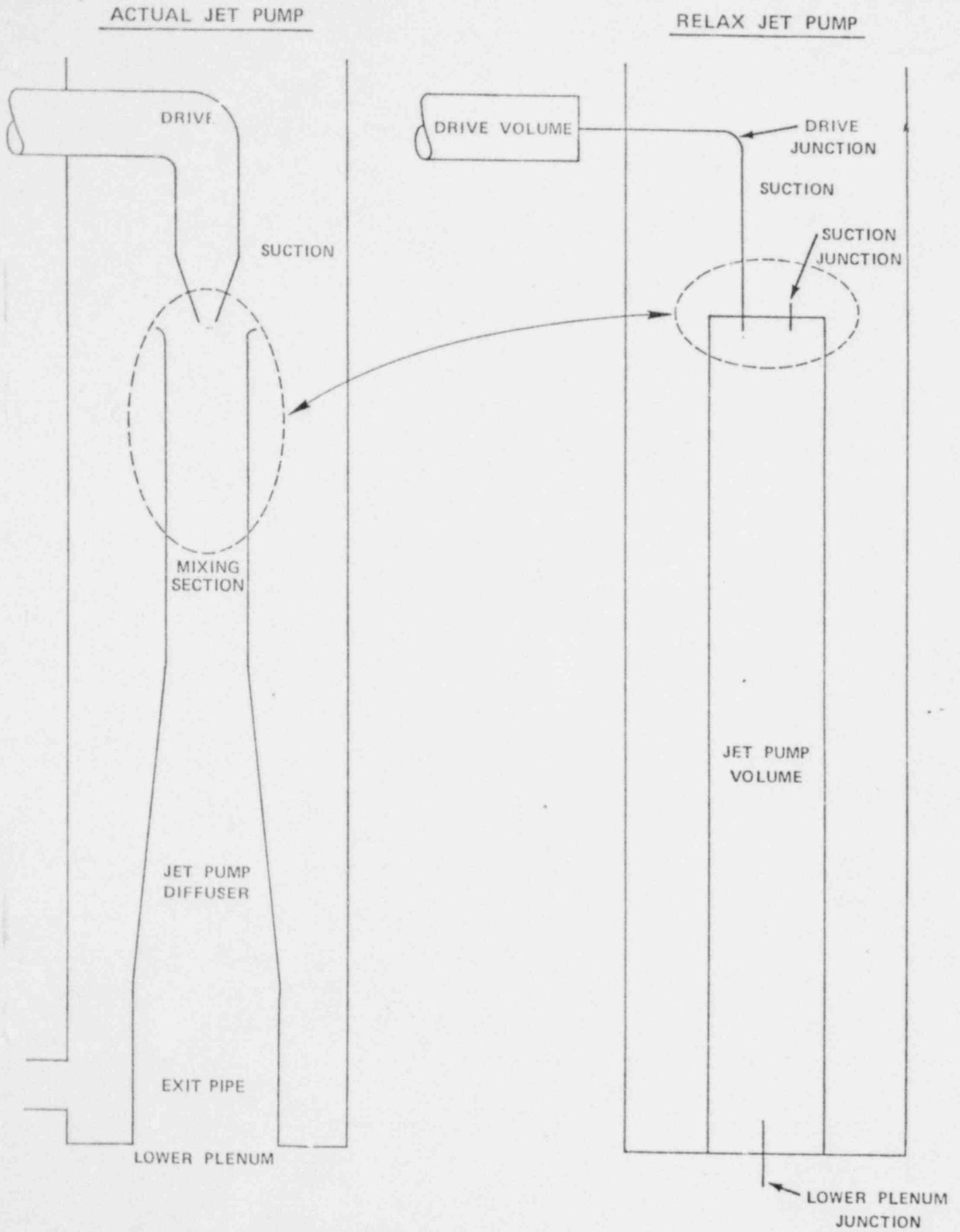


FIGURE 3.2 RELAX MODEL OF AN ACTUAL JET PUMP

FIGURE 3.3 NODING FOR JET PUMP MIXING SECTION AND
ILLUSTRATION FOR TYPE 3+ FLOW.

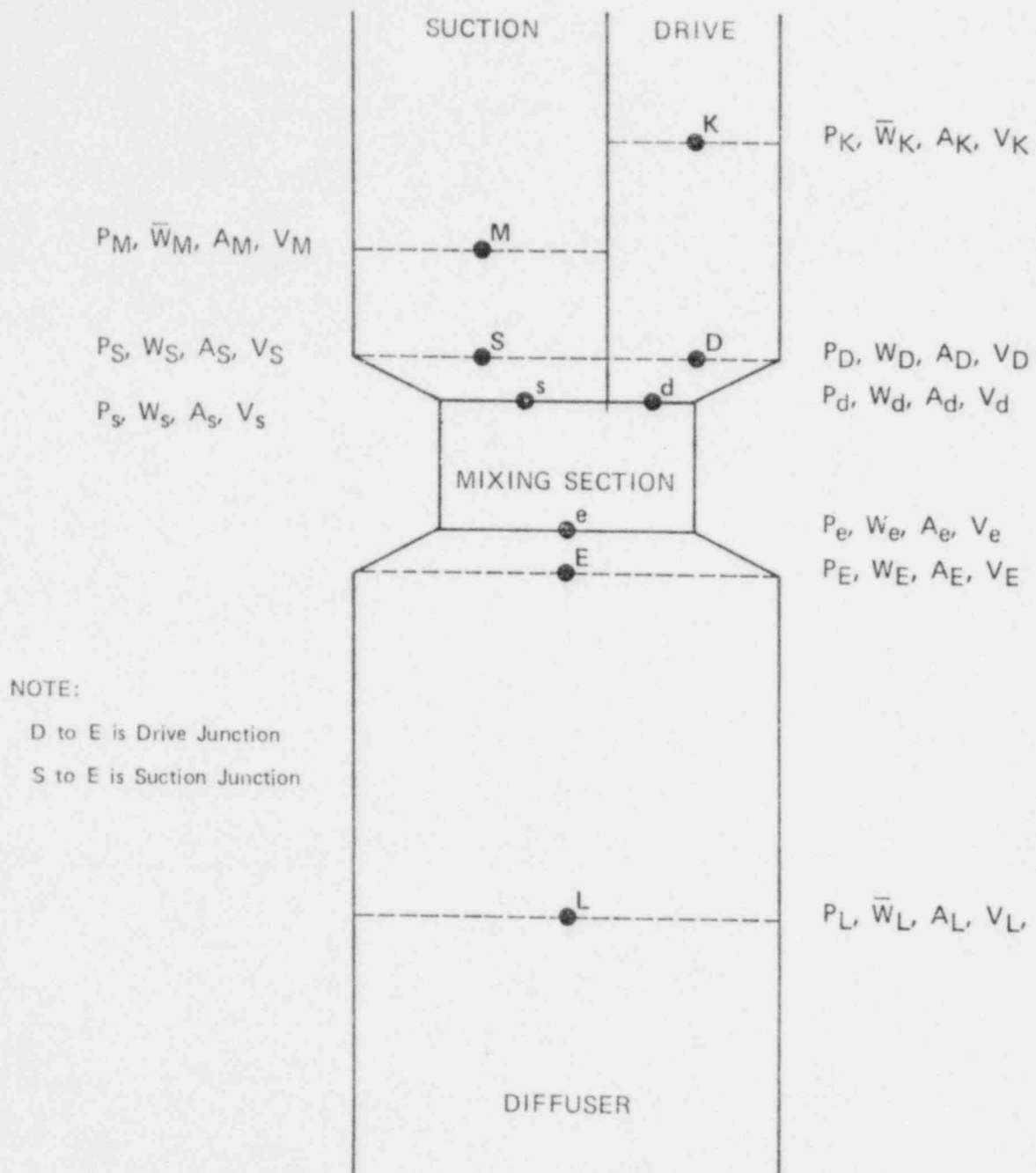


FIGURE 3.4 LOCATION OF VARIABLES IN JET PUMP MODEL.

FIGURE 3.5 VARIABLE PLACEMENT FOR THE MULTINODE MIXING SECTION.

FIGURE 3.6 JET PUMP LOSS COEFFICIENTS OBTAINED FROM EG&G FLOW TESTS.

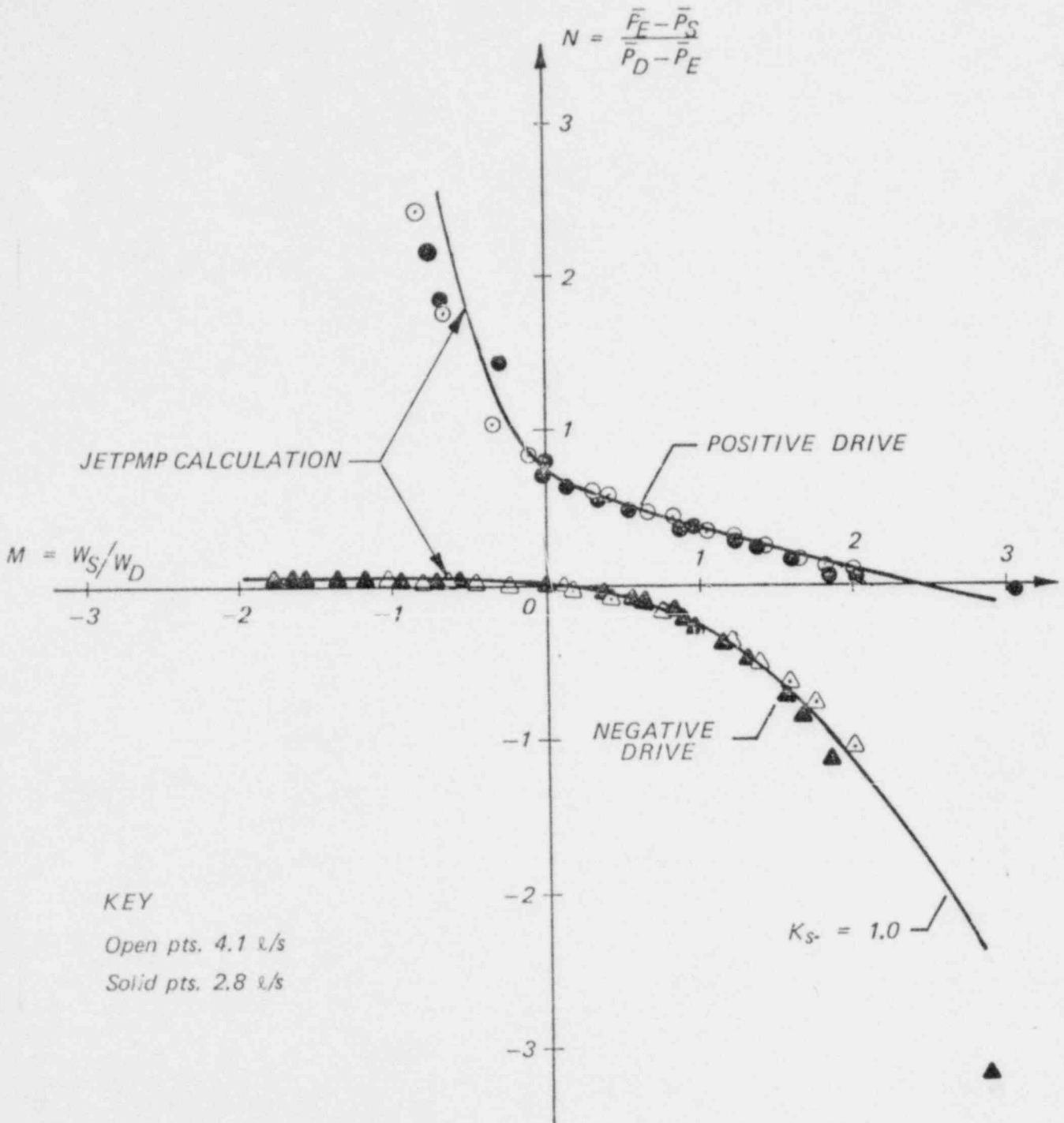


FIGURE 3.7 COMPARISON OF EXPERIMENTAL AND CALCULATED M-N CURVE FOR EG&G JET PUMP TESTS⁽²⁴⁾

4.0 HEAT TRANSFER REGIMES

Three heat transfer regimes were added to provide improved system blowdown heat transfer predictions: condensation, natural convection and pool film boiling. These regimes are further discussed in the section 4.1

In addition, all recent updates⁽¹⁹⁾ that have been made to the approved⁽²⁾ NRC version of RELAP4 from which RELAX was developed (ENC 28B)⁽¹⁾ have been incorporated into RELAX. Thus RELAX is consistent with the current ENC version of RELAP4. Section 4.2 discusses these RELAP4 updates in detail. Most of these RELAP4 updates involved the same heat transfer regimes discussed in Section 4.1.

4.1 HEAT TRANSFER CORRELATIONS

Heat transfer correlations were added to RELAX so that isolation condenser performance could be modeled (if necessary), dual cycle BWR plants with steam generators could be better modeled and core thermal response could be improved for low flow/low quality conditions.

4.1.1 Condensation

The condensation regime that was included in RELAX consists of a turbulent and a laminar condensation correlation. When the surface temperature of a heat slab is below T_{sat} , $T_{bulk} \geq T_{sat}$, and the quality in the adjoining volume is greater than zero, then the condensation regime is activated. For turbulent conditions the correlation of Z.L. Miropolskiy⁽²⁵⁾ is used:

$$h_c = 0.023 \left(\frac{k_f}{D} \right)^{.8} Re_f^{.4} Pr_f \left[1 + X \left(\frac{\rho_f}{\rho_g} - 1 \right) \right]^{.5}$$

where:

- h_c = condensation coefficient
- k_f = liquid thermal conductivity
- D = hydraulic diameter
- Re_f = liquid Reynolds number
- Pr_f = liquid Prandtl Number
- X = volume average quality
- ρ_f = liquid density
- ρ_g = vapor density

This correlation was developed for condensation of steam inside tubes. The correlation is valid for anticipated blowdown pressures (60-3000 psia, 0.41-20.7 MPa) and mass fluxes (37.9-379 lb_m/ft² sec, 17.2-172 kg/m² sec). At lower mass fluxes, the correlation conservatively underpredicts data as the effect of gravity in condensation films flows is not considered. For these lower mass fluxes, the laminar condensation correlation is used.

The laminar condensation correlation is the classical Nusselt⁽²⁶⁾ laminar condensation correlation for horizontal tubes as modified for the presence of residual condensate on the inside of the tubes.

$$h = F \left[\frac{k_f^3 \rho_f^2 g H_{fg}}{\mu_f D (T_{sat} - T_w)} \right]^{1/4}$$

where properties are evaluated at the average film temperature, and:

- D = inside diameter of tube
- H_{fg} = enthalpy difference between saturated steam and subcooled liquid in the film

F = factor which accounts for the reduction in heat transfer due to the residual liquid in the bottom of the tube. F was developed from a least squares fit to a model given in Collier⁽²⁶⁾.

$$F = 0.43 + 3.37\alpha - 18.2\alpha^2 + 53.0\alpha^3 - 77.1\alpha^4 + 54.1\alpha^5 - 14.4\alpha^6$$

$(T_{sat} - T_w)$ = subcooling temperature of the wall

α = void fraction

μ_f = dynamic viscosity of liquid

The turbulent heat transfer coefficient is used except where its value unrealistically extrapolates below the laminar coefficient value.

4.1.2 Natural Convection

As discussed in Reference (27), turbulent conditions are usually encountered in water systems under natural circulation conditions. For completeness, both turbulent and laminar natural convection heat transfer correlations were included. The turbulent natural convection correlation contained in the WREM⁽²¹⁾ version of RELAP4-EM FLOOD was incorporated into RELAX. To cover laminar conditions, the laminar natural convection heat transfer correlation of Kreith⁽²⁸⁾ was added. The transition between these correlations is chosen where these two heat transfer correlations intersect on a Nusselt Number/Prandtl-Grashof Number plot.

The natural convection regime is allowed when the volume fluid conditions is single phase and the mass flux is less than 200,000 lb/ft.²hr. (271 Kg/m².sec). Both the forced convection heat transfer coefficient and the natural convection heat transfer coefficient are computed and the larger value selected.

4.1.3 Pool Film Boiling

A forced convection boiling correlation currently exists in RELAP4 and RELAX; however, at low flows, this correlation extrapolates to an unrealistically low value. To cover this low flow range, the modified Bromley pool film boiling correlation has been included in RELAX. This correlation is justified for reactor plant application in Reference (29).

The pool film boiling regime heat transfer coefficient (modified Bromley⁽³⁰⁾) is incorporated as follows:

$$h = h_b + h_r$$

where

$$h_b = 0.62 \left[\frac{k_g^3 (\rho_f - \rho_g) \rho_g H_{fg}}{\mu_g (T_w - T_{sat}) L_H} \right]^{1/4}$$

k_g and μ_g are the gas thermal conductivity and dynamic viscosity respectively and the length parameter is taken from Helmholtz instability considerations as

$$L_H = 16.2 \left[\frac{c^4 H_{fg}^3 \mu_g^5 g_c^4}{g^5 \rho_g (\rho_f - \rho_g)^5 k_g^3 (T_w - T_{sat})^3} \right]^{1/11}$$

h_r is the radiation heat transfer coefficient (31) defined as:

$$h_r = \sigma_r \epsilon_w \frac{(T_w^4 - T_{sat}^4)}{(T_w - T_{sat})}$$

where the wall emittance (ϵ_w) takes on the accepted value (32) of 0.67 for oxidized zirconium.

This film boiling regime is applied after the 300°F wettable

surface lockout has been reached and when the film boiling heat transfer coefficient is greater than the value of the extrapolated forced convection film boiling heat transfer coefficient.

4.1.4 Convective Boundary Condition - Mixture Level Interaction

The heat slab convective boundary condition was improved by considering the elevation of the adjacent volume mixture level. Whenever a mixture level exists along a heat slab, the convection heat transfer coefficient is determined by a weighting of the covered and uncovered heat transfer coefficients by the respective covered and uncovered slab surface areas.

4.2 RELAP4 UPDATES

All RELAP4 updates that have been made to the approved version (ENC28B) from which RELAX was developed have been incorporated into RELAX. These updates are discussed in Reference (19), and the changes which could impact computed results are summarized below:

- An improved numerical iteration scheme for initializing the heat slab stored energy was incorporated. This modification only changed the numerical scheme and did not alter any physical model (such as the fuel/clad thermal expansion model or the gap conductive model); stored energy in the fuel is still determined from the approved GAPEX⁽³³⁾ model. A plant calculation confirmed a negligible impact of this change on PCT (<2F°).
- The changes described in Section 4.1.1 and 4.1.2 were previously incorporated into RELAP4.

5.0 NOMENCLATURE5.1 NOMENCLATURE OF DRIFT FLUX SECTION (SECTION 2)

- A_i = flow area of volume i
 C = Kutateladze or Wallis constant
 C_0 = distribution parameter in Zuber-Findlay equation
 D = hydraulic diameter
 f_i = interfacial friction factor
 G = total mass flux
 g = acceleration due to gravity
 g_c = gravitational conversion factor
 h_{g_j}, h_{l_j} = local saturated gas and liquid enthalpy at junction j
 h_j = local enthalpy at junction j
 j = volumetric flux of gas-liquid mixture
 j_g, j_f = volumetric fluxes of gas and liquid, respectively
 l_i = flow length of volume i
 m = Kutateladze or Wallis constant
 Q_i = rate of heat energy transferred into volume i
 U_i = total fluid internal energy within volume i
 v_{gj}^P = v_{gj} based on flow pattern
 v_{gj}^F = v_{gj} based on flooding
 v_{gj} = local mean drift velocity
 v_j = local fluid velocity at junction j
 v_g = local gas velocity

\bar{V}_{gj} = mean transport drift velocity

v_m = mixture center-of-mass velocity

\bar{W}_i = average mass flow in volume i

W_j = local flow at junction j

W_{gj}, W_{lj} = local gas and liquid flow at junction j

$z_j - z_i$ = elevation change from the center of mass of volume i
to junction j

Greek

α = void fraction

α^F = void fraction corresponding to local flooding

ρ_i = average fluid density in volume i

ρ_g, ρ_f = saturated densities of gas and liquid, respectively

ρ_m = mixture density

$\Delta\rho = \rho_f - \rho_g$

σ = surface tension

μ_f = liquid viscosity

ξ = ratio of wetted perimeters of interface to wall

5.2 NOMENCLATURE OF JET PUMP SECTION (SECTION 3)

- A = area
- D = diameter
- F = force
- g = gravitational acceleration
- H = elevation head
- I = volume flow inertia
- K = loss coefficient
- L = left side
- M = ratio of flows (see Equation 3.1)
- N = ratio of total pressure differences (see Equation 3.2)
- P, P' = pressure, static
- P_w = wetted perimeter
- P_e^{*} = total pressure in exit region outside of mixing region
- P_d^{*} = total pressure in drive region outside of mixing region
- P_s^{*} = total pressure in suction region outside of mixing region
- ΔP = pressure drop
- R = right side
- t = time
- U, U' = longitudinal velocity
- U^{*} = donor velocity
- V = transverse velocity
- v = velocity

- W = total mass flow rate
 \bar{W} = total mass flow rate averaged over volume
 W_d = drive flow rate
 W_s = suction flow rate
 x = longitudinal position
 y = transverse position
 v = specific volume
 ρ = density

6.0 REFERENCES

1. "Safety Evaluation by USNRC on RELAP4-EM/ENC28B," (ENC Letter dated October 30, 1978), Forwarded by NRC Letter from T. A. Ippolito to W. S. Nechodom dated March 30, 1979.
2. "Description of RELAP4/ENC28B," ENC Letter from G. F. Owsley to D. F. Ross (USNRC), dated October 30, 1978.
3. N. Zuber and J. Findlay, "Average Volumetric Concentration in Two-Phase Flow Systems," Trans. ASME J. Heat Transfer, Ser. C., 87, 453-468 (1965).
4. C. W. Hirt and J. C. Romero, "Application of a Drift Flux Model to Flashing in Straight Pipes," LA-6005, MS, US-78c (July 1975).
5. R. D. Kelly, R. S. Dougall and B. J. Contineau, "Application of Drift Flux to Loss-of-Coolant Analysis," ASME Winter Annual Meeting, New York, N.Y., (November 17-22, 1974).
6. H. W. Vea and R. T. Lahey, Jr., "An Exact Analytical Solution of Pool Swell Dynamics During Depressurization by the Method of Characteristics," RPI (to be published).
7. W. C. Panches, "MAYU04: A Method to Evaluate Transient Thermal Hydraulic Conditions in Rod Bundles," GEAP-23517 NRC-2, a NRC-EPRI-GE Cooperative R&D Report, (March 1976).
8. M. Ishii, "One-Dimensional Drift Flux Model and Constitutive Equations for Relative Motion Between Phases in Various Two-Phase Flow Regimes," ANL-77-47.
9. K. Ohkawa and R. T. Lahey, "The Analysis of Proposed BWR Inlet Flow Blockage Experiments in PBF," NES-496, RPI Topical Report, (December 1978).
10. M. Ishii, T. C. Chawla and N. Zuber, "Constitutive Equation for Vapor Drift Velocity in Two-Phase Annular Flow," AICLÉ Journal, Vol. 22, No. 2, March 1976.
11. N. Zuber and F. W. Staub, "An Analytical Investigation of the Transient Response of the Volumetric Concentration in a Boiling Forced-Flow System," Nuclear Science and Engineering, 30, 268-278 (1967).
12. "RELAP4/MOD5: A Computer Program for Transient Thermal Hydraulic Analysis of Nuclear Reactors and Related Systems User's Manual," 3 Volumes, ANCR-NUREG-1335, Idaho National Engineering Laboratory, (September 1976).

13. Transient Two-Phase Flow, Proceedings of the CSNI Specialists Meeting, August 3-4, 1976, Toronto, Vol. 1, 316-350, (RELAP-UK Code Description), (1976).
14. "CEFLASH-4A: A Fortran-IV Digital Computer Program for Reactor Blowdown Analysis," CENPD-133 (August 1974).
15. ECCS Subcommittee Meeting, USNRC, Washington, D. C., Tuesday, June 15, 1976, (Westinghouse Overview of UHI Model)(1976).
16. NUREG/CR-0063, LS-7279-MS, Vol. I, "TRAC-PI: An Advanced Best-Estimate Computer Program for FWR LOCA Analysis, Vol. I: Methods, Models, User Information, and Programming Details," Los Alamos Scientific Laboratory (June 1978).
17. A. W. Bennett, et al., "Flow Visualization Studies of Boiling at High Pressure," AERE-R 4874, (1965).
18. Quarterly Progress Report Jan. 1-March 31, 1978, NUREG/CR-0147 BMI-2003, Steam-Water Mixing and System Hydrodynamics Program, Task 4 (1978).
19. "ECCS Evaluation of Dresden I Using the Exxon Nuclear Company WREM-Based Non-Jet Pump Evaluation Model," XN-NF-79-95(NP), Rev. 1, dated April 1980.
20. ANCR-1127, Rev. 1, "RELAP4 - A Computer Program for Transient Thermal Hydraulic Analysis," Aerojet Nuclear Company, (March 1975).
21. NUREG-75/056, "WREM: Water Reactor Evaluation Model (Revision 1)," (May 1975).
22. G. B. Wallis, "One-Dimensional Two-Phase Flow," McGraw-Hill, Inc., New York, N. Y., (1969).
23. F. H. Harlow and A. A. Amsden, "A Numerical Fluid Dynamics Method for all Flow Speeds," J. Computational Physics, Vol. 8, 197-213, ((1971).
24. H. S. Crapo, "One-Sixth Scale Model BWR Jet Pump Test," EGG-LOFT-5063, LTR 20-105, November 29, 1979.
25. Miropolskiy, Z. L., Shneerova, R. I., and Ternakova, L. M., Volume III, Int. Heat Transfer Conf., Japan, Cs. 1.7 (1974).
26. Convective Boiling and Condensation, John G. Collier, McGraw-Hill Book Co., 1972.

27. Brown, A. I. and Marco, S. M., Introduction to Heat Transfer, McGraw-Hill Book Co., Third Edition, 1958, page 165.
28. Kreith, F., Principles of Heat Transfer, International Textbook Company, Fourth Printing, 1961, page 306.
29. Analytical Model for LOCA in Accordance with 10 CFR 50 Appendix K: Amendment No. 1, Calculation of Low Flow Film Boiling Heat transfer for BWR LOCA Analysis, NEDO-20566-1, General Electric Co., dated January 1977.
30. Bromley, L. A., Heat Transfer in Stable Film Boiling, Chem. Eng. Progr. 46, 22-227 (1950).
31. Giedt, W. H. Principles of Engineering Heat Transfer, D. Van Nostrand Co., Inc., (1957).
32. Exxon Nuclear Company, "HUXY: A Generalized Multirod Heatup Code with 10 CFR 50 Appendix K Heatup Option - User's Manual," XN-CC-33(A), Revision 1, November 1, 1975.
33. Exxon Nuclear Company, "GAPFX. A Computer Program for Predicting Pellet-to-Cladding Heat Transfer Coefficients," XN-73-25, August 13, 1973.
34. XN-NF-77-15, "Verification of RELAP4-EM (ENC/22) By Comparison With Measured TLTA Blowdown Data for Test 4906," August 1977.
35. GEAP-23592, "BWR Blowdown/Emergency Core Cooling Program, Preliminary Facility Description Report for the BD/ECCIA Test Phase," December 1977.

APPENDIX A

VERIFICATION: RELAX PREDICTION OF EXPERIMENTAL
BWR SYSTEM BEHAVIOR (TLTA)

Post-test predictions using RELAX of a recent TLTA Test (#6007) which simulated a JP-BWR blowdown are presented. The comparison between prediction and experimental data is typical of the ability of RELAX to predict BWR blowdown responses and supports its use as the JP-BWR blowdown evaluation model.

The RELAX code was used in the evaluation model (EM) mode except that actual simulated fuel assembly power was used and the critical flow in the subcooled region was described by the Henry-Fauske Model. The EM Moody critical flow model (with a 0.8 multiplier) was used for saturated conditions. Since uncertainties in break flow is covered by a break size spectrum in licensing calculations, this small deviation from the EM critical flow is justified.

TLTA is a scaled simulation of a jet pump BWR and has been upgraded to better simulate modern JP plants⁽³⁴⁾. The test run chosen (#6007) for this comparison was made with the upgraded facility. Nodalization and other RELAX inputs were closely related to those of the Example Problem in Volume 2 of this document as much as geometry and test conditions would allow.

Calculated and experimental steam dome pressures are compared in Figure A-1. Very good agreement is shown; the small variations that do occur are within the uncertainties that exist in subcooled critical flow which are covered by break size spectrum analyses in licensing calculations.

RELAX calculated core inlet flow is compared to the measured flow in Figure A-2. Very good agreement is shown in both magnitudes and key event times.

In both the predictions, the 0 to 7 second coastdown, the jet pump uncover (7-8 seconds), the low (even reverse) flow window period (8-11 seconds) and the core flow surge due to lower plenum flashing (11 seconds and on) are evident. The RELAX calculation was terminated early since some of the experimental data such as core flow is not valid after 14 seconds.

TLTA tests have shown that significant liquid inventory remains in the lower plenum during blowdown. Comparison of predicted and measured liquid mass inventories in the lower plenum is shown in Figure A-3. Again, good agreement between RELAX and data is evident.

This excellent agreement between RELAX predictions and representative TLTA data justifies the improvements made to RELAX. These figures show better agreement than were obtained with RELAP4⁽³⁵⁾ on TLTA data. Thus, RELAX is capable of adequately predicting blowdown phenomena in jet pump BWR plants.

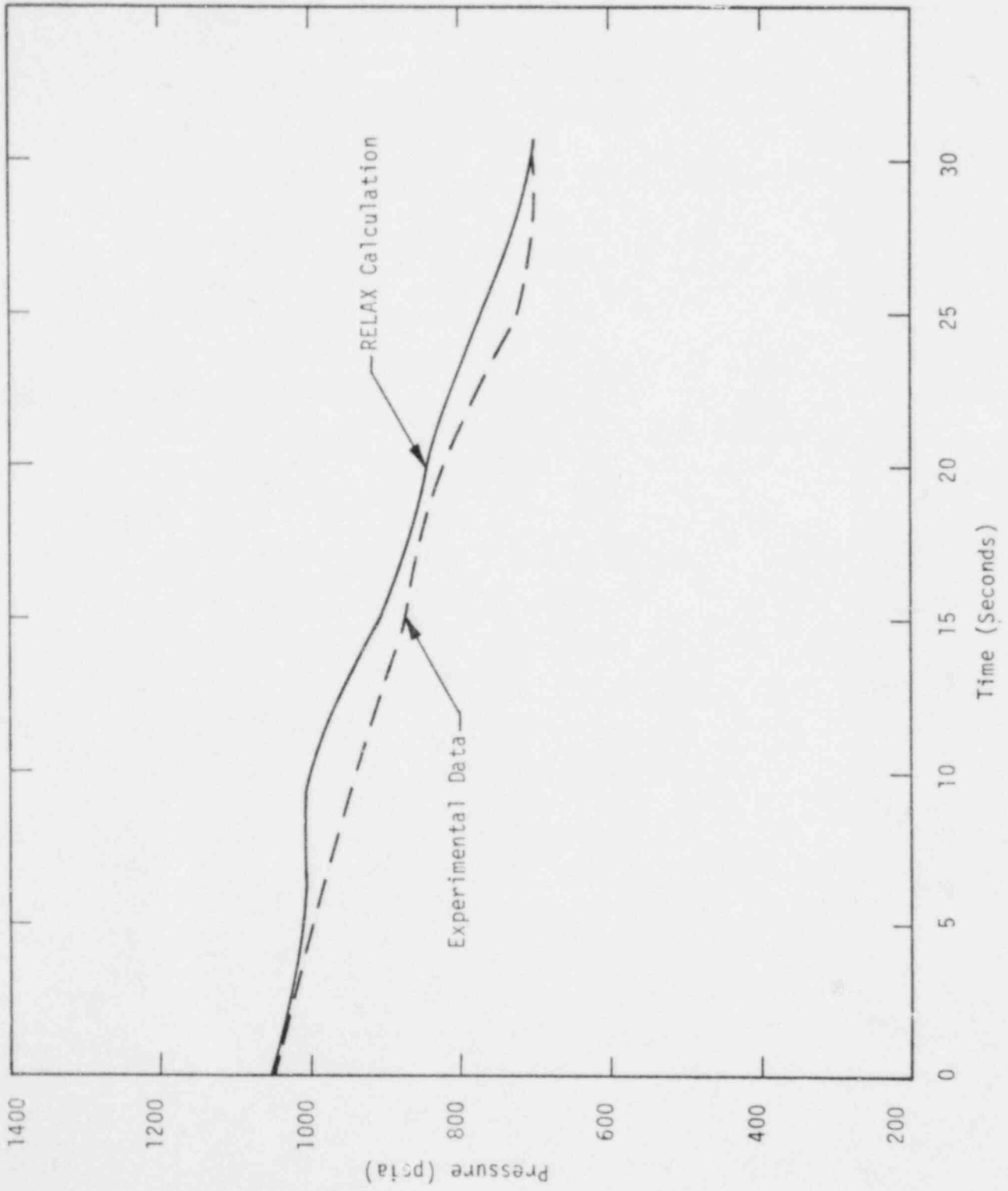


Figure A-1 Steam Dome Pressure - TLTA Test 6007 Run 26

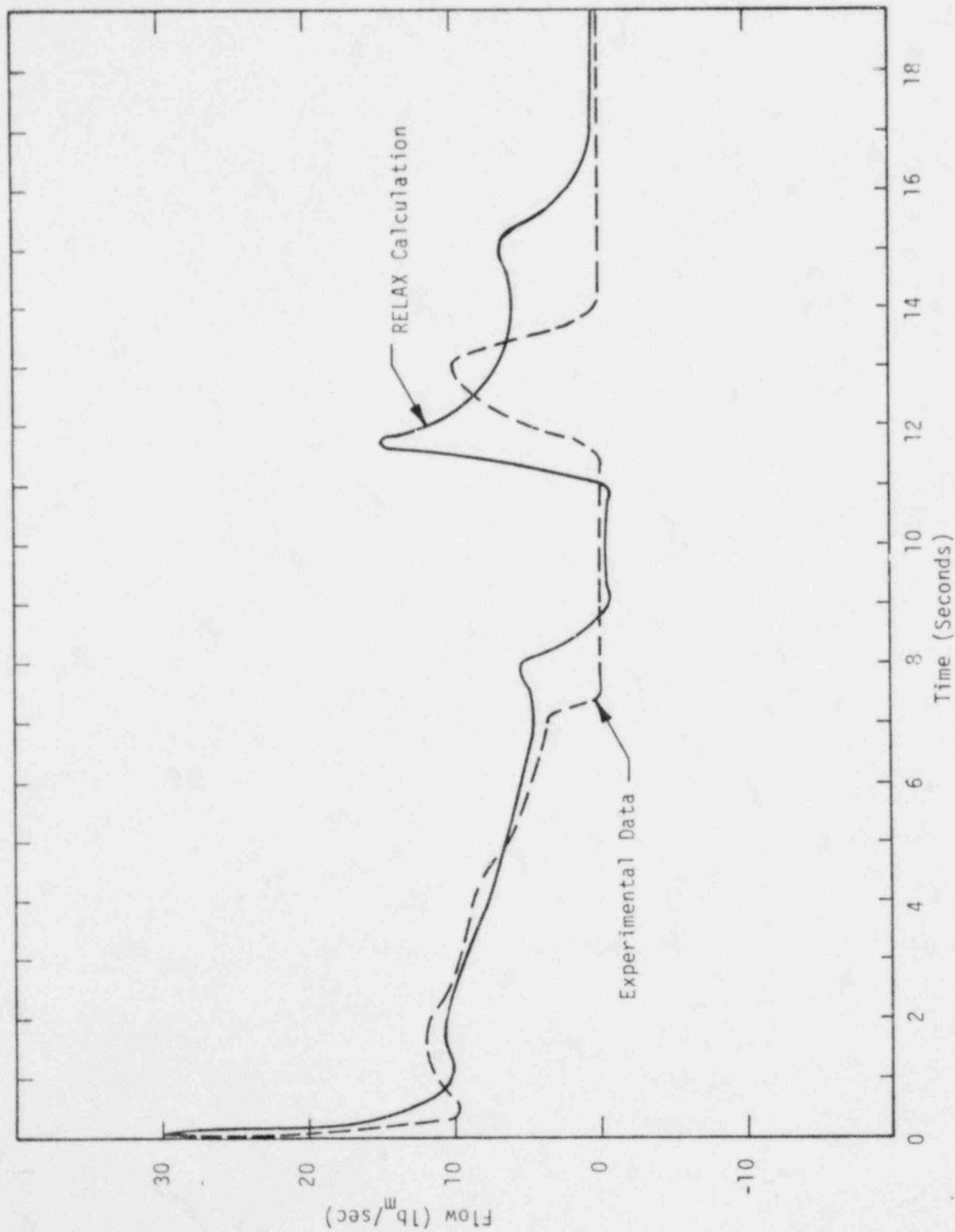


Figure A-2 Core Inlet Flow - TLTA Test 6007 Run 26

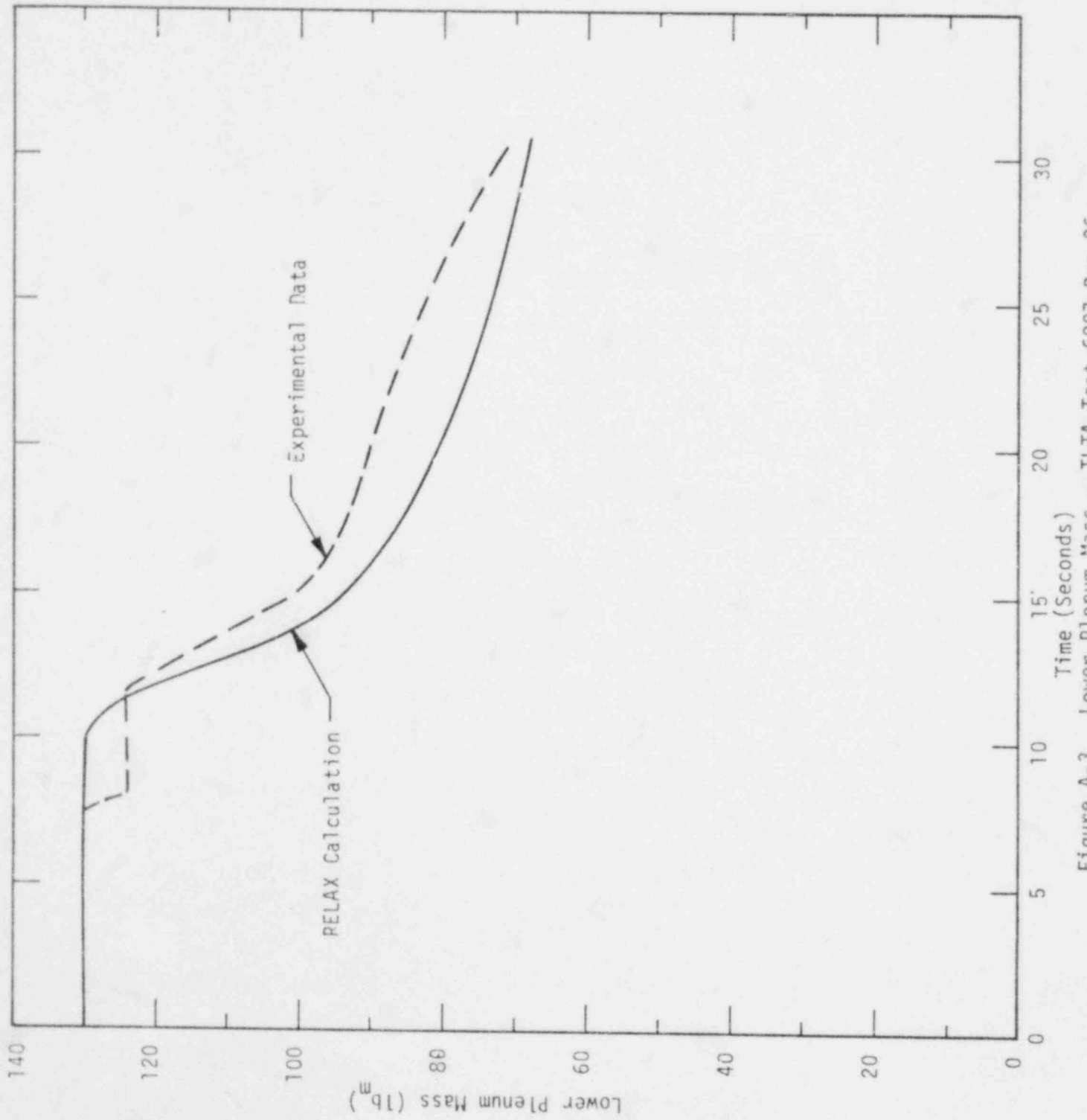


Figure A-3 Lower Plenum Mass - TLTA Test 6007 Run 26

XN-NF-80-19(NP)
Volume 2A

07/31/80

RELAX: A RELAP4 BASED COMPUTER CODE
FOR CALCULATING BLOWDOWN PHENOMENA

Distribution

RE Collingham
DC Kolesar
GF Owsley

USNRC/GF Owsley (20)

Document Control (5)